AD-A051 077 WEAPONS RESEARCH ESTABLISHMENT SALISBURY (AUSTRALIA) F/G 4/1
DAYTIME OBSERVATIONS OF LOWER THERMOSPHERIC WIND PROFILES AT WO--ETC(U)
APR 77 K H LLOYD, C H LOW, A D HIND

UNCLASSIFIED WRE-TR-1809(W) NL

| OF |

AD
A051077

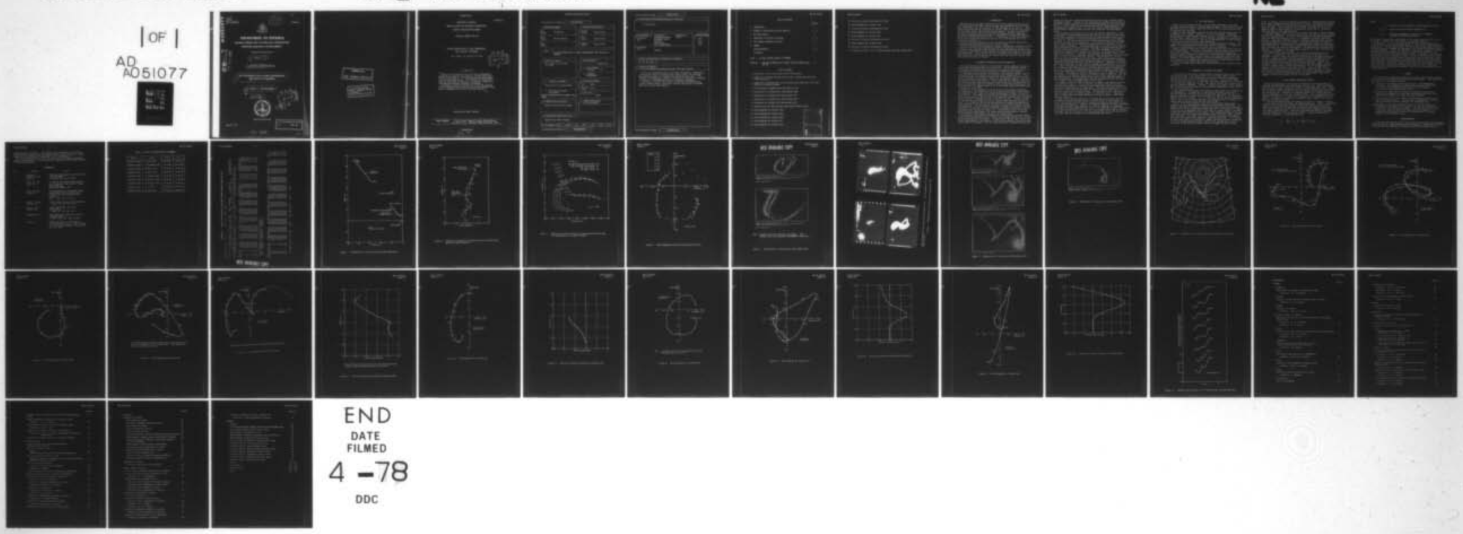

END
DATE
FILMED
4 -78
DDC

AD A051077

14

WRE-TR-1809 (W)

12

AR-000-553

AD NO.
DDC FILE COPY

DEPARTMENT OF DEFENCE

DEFENCE SCIENCE AND TECHNOLOGY ORGANISATION

WEAPONS RESEARCH ESTABLISHMENT

SALISBURY, SOUTH AUSTRALIA

11 Apr 77

9 TECHNICAL REPORT 1809 (W)

6 DAYTIME OBSERVATIONS OF LOWER THERMOSPHERIC WIND PROFILES AT WOOMERA

10 K.H. LLOYD, C.H. LOW and A.D. HIND

12 38p.

DDC
MAR 10 1978
F

Approved for Public Release

COPY No. 84

© Commonwealth of Australia
APRIL 1977

371 700

APPROVED

FOR PUBLIC RELEASE

THE UNITED STATES NATIONAL
TECHNICAL INFORMATION SERVICE
IS AUTHORISED TO
REPRODUCE AND SELL THIS REPORT

UNCLASSIFIED

AR-000-553

DEPARTMENT OF DEFENCE

DEFENCE SCIENCE AND TECHNOLOGY ORGANISATION

WEAPONS RESEARCH ESTABLISHMENT

TECHNICAL REPORT 1809 (W)

DAYTIME OBSERVATIONS OF LOWER THERMOSPHERIC WIND PROFILES AT WOOMERA

K.H. Lloyd, C.H. Low and A.D. Hind

DDC
MAR 10 1978
F

SUMMARY

Profiles of the daytime wind in the lower thermosphere, determined by observing the release of lithium vapour from a rocket, are presented. The observed profiles are compared with predicted tidal winds. The influence of thermospheric winds on ionisation distribution is discussed in relation to simultaneously observed ionospheric parameters.

An outline is given of the analysis of the data obtained from the daytime lithium scanners, particular attention being given to problems which arise in the data analysis.

Approved for Public Release

POSTAL ADDRESS: The Director, Weapons Research Establishment, Box 2151, G.P.O., Adelaide, South Australia, 5001.

UNCLASSIFIED

page - A -

DOCUMENT CONTROL DATA SHEET

Security classification of this page: UNCLASSIFIED

1 DOCUMENT NUMBERS	
AR Number:	AR-000-553
Report Number:	WRE-TR-1809(W)
Other Numbers:	

2 SECURITY CLASSIFICATION	
a. Complete Document:	Unclassified
b. Title in Isolation:	Unclassified
c. Summary in Isolation:	Unclassified

3 TITLE

DAYTIME OBSERVATIONS OF LOWER THERMOSPHERIC WIND PROFILES AT WOOMERA

4 PERSONAL AUTHOR(S):

K.H. Lloyd, C.H. Low and A.D. Hind

5 DOCUMENT DATE:

April 1977

6 6.1 TOTAL NUMBER OF PAGES 41

6.2 NUMBER OF REFERENCES: 7

7 7.1 CORPORATE AUTHOR(S):

Weapons Research Establishment

7.2 DOCUMENT (WING) SERIES AND NUMBER

Weapons Research and Development Wing 1809

8 REFERENCE NUMBERS

a. Task: 61/3

b. Sponsoring Agency: RD73

9 COST CODE:

330897

10 IMPRINT (Publishing establishment):

Weapons Research Establishment

11 COMPUTER PROGRAM(S) (Title(s) and language(s))

12 RELEASE LIMITATIONS (of the document):

Approved for Public Release

12.0	OVERSEAS	NO		P.R.	1	A		B		C		D		E	

Security classification of this page: UNCLASSIFIED

Security classification of this page: UNCLASSIFIED

13 ANNOUNCEMENT LIMITATIONS (of the information on these pages):

No limitations

14 DESCRIPTORS:

a. EJC Thesaurus Terms

Thermosphere
Atmospheric models
Sounding rockets
Daylight
Observation
Wind (meteorology)
Condensation trails

b. Non-Thesaurus Terms

Woomera

15 COSATI CODES:

0401
0402
0704

16 LIBRARY LOCATION CODES (for libraries listed in the distribution):

SW SR SD AACA NL

17 SUMMARY OR ABSTRACT:
(if this is security classified, the announcement of this report will be similarly classified)

Profiles of the daytime wind in the lower thermosphere, determined by observing the release of lithium vapour from a rocket, are presented. The observed profiles are compared with predicted tidal winds. The influence of thermospheric winds on ionisation distribution is discussed in relation to simultaneously observed ionospheric parameters.

An outline is given of the analysis of the data obtained from the daytime lithium scanners, particular attention being given to problems which arise in the data analysis.

Security classification of this page: UNCLASSIFIED

TABLE OF CONTENTS

LIST OF FIGURES

ACCESSION for
NTIS White Section ☑
DDC Buff Section ☐
UNANNOUNCED ☐
JUSTIFICATION
BY
DISTRIBUTION/AVAILABILITY CODES
Dist. SPECIAL
A

1. INTRODUCTION

Determination of the upper atmospheric wind profile between 80 and 200 km by observing the drift of vapour trails released from sounding rockets has become well established, since its inception in 1958 (Bedinger et al.,(ref.1)). Until recently the technique was restricted to twilight, when the sky was dark enough for the sunlit trail to be observed from the ground. In order to extend the period of observation, and to provide data during daylight hours when many ionospheric phenomena are more evident, an instrument to discriminate lithium against the daylight sky has been built. A description of this instrument has been given by Hind and Lloyd(ref.2), and the first data provided by it are reported in reference 3.

This Note presents and discusses all the profiles of daytime thermospheric winds which have been observed since the initial report.

Section 2 discusses the data analysis methods, and Section 3 presents the data. In Section 4 these data are compared with profiles determined at twilight, and in Section 5 the calculated redistribution of ionisation expected for these wind profiles is compared with observed ground based observations made by an ionosonde and magnetometer. The positions of these instruments with respect to the range-head, along with those of the daytime scanner observing sites and typical rocket trajectories are given in figure 1.

2. METHODS OF OBSERVATION AND DATA ANALYSIS

The construction and operation of the daylight lithium scanning detector has already been described by Hind and Lloyd(ref.2). The instruments operated satisfactorily throughout their three years of operation, and in the course of their operation only a few minor modifications needed to be introduced.

The main modification involved automatically recording the voltage supply to the potentiometers which monitor the position of the scanning mirrors. These reference voltages are recorded between frames during reset, and are processed in the same manner as the monitor voltages so that drifts anywhere in the recording system are taken into account. It was found that the reference voltage on the final processed output had negligible drift during the trial and during the angular calibrations (which took about 45 minutes), but that differences in output equivalent to an angular change of up to two degrees could occur between the trial and the calibrations.

Originally, it was intended to use the stars for the angular calibrations, but difficulties in distinguishing the star data from spike noise (and problems of clouding in of the site), necessitated abandoning this method in favour of using the sun. The azimuth and elevation of the mount on successive calibration points were changed, so that a series of calibrations were made with the image of the sun lying in a different position in the field of view. Thirteen calibration points were used, chosen to lie in a matrix evenly covering the field of view. The accuracy of the calibration procedure was checked by comparing the actual position of the sun with the sun's position calculated from the calibration parameters. The last column in Appendix I, which is an example of angular calibration calculations, shows that the mean difference between the actual and recomputed sun's positions is about 0.3^{o}. Contributions to this error stem equally from the signal output, the scanner mount azimuth/elevation readings, and estimation of the centre of the sun on the output trace.

The accuracy of this method of determining the wind profile has been checked against the proven method using F24 cameras, by observing lithium trails released by two Corella rockets at twilight. A comparison of the two sets of data also enabled improvements in the analysis of data from the daytime scanner to be made. As described in reference 2, the final wind profile was originally determined by

feeding the data into a function minimisation routine using a powerful method developed by Powell. However, it was found that the routine could converge on subsidiary minima, instead of the true minimum represented by the correct wind profile. Also, to find the true minimum required much hand manipulation, and was demanding in computer time. In its place a more suitable technique was evolved which yielded consistent profiles in a relatively straight forward manner.

The principle of the method was to assign altitudes to observations of the lithium trail at similar times from the two sites so that they were consistent. As an example, consider the data taken from one frame recorded at each site (a "frame" is a complete set of scans through the field of view, as for example, in figure 8). The data consist of the azimuth and elevation of points along the trial, and the time of observation. If we knew the altitude of each data point at one of the sites, the North and West position of this point in the trail could be calculated. Since the trajectory of the rocket (which gives the initial position of the trail) is known from radar, it would enable the drift velocity of the trail to be calculated. With this knowledge, it would be possible to calculate where in space the trail was, at the time data was being taken at the other site. From this, the elevation and azimuth of the trail from that site could be calculated, and the results should agree with the observed data. In fact, we do not know the altitude. What is done is to assign different sets of altitudes to the data at both sites, and see which set gives consistent agreement between the reprojected azimuth and elevation (calculated using the method explained above) and the observations. Generally, constraints can be put on altitude, so that the first estimate was generally within 5 to 10 km. These constraints are the rocket apogee (known from the radar trajectory), the altitude of well defined kinks in the trail (which could be triangulated directly), the lowest altitude below which lithium was rapidly oxidised (about 85 km) and comparison of the earliest observations with the radar trajectory of the rocket. An example of this last technique is given in figure 2. This was an observation of a downleg release from a Skylark rocket, and the distance of the observing sites from the release did not give a large subtended angle, i.e. poor triangulation. The figure shows that the altitude where the loop forms (c.f. figure 3) can be assigned within 10 km at worst.

An example of the new method of analysis is shown for the difficult Skylark 1271 release in figure 3. It is seen that the highest altitude has been assigned an altitude 10 km too high, the altitudes were correct in the middle range, but further down were too high again. The graph also shows that at low altitudes the data from the two sites are inconsistent with each other, i.e. one or other or both sets of data are wrong. The trail was in fact very faint at these altitudes and it was hard to pick it out from the noise. Comparisons such as figure 3 have the added advantage of acting as a guide to show which data are incorrect.

Figure 4 shows the wind velocities calculated for trial Lorikeet 2013 for which data were obtained from only one site (the other site was clouded in). In this case there is no check on the assigned altitudes by reprojection to the other site and comparison. However, the velocity hodograph is fairly insensitive to assigned altitudes, the problem is to assign altitudes to this hodograph. Even when data are obtained from both sites, it is preferable to quote the accuracy of the derived wind profile as a mean error in altitude rather than in velocity. A typical value for this error is ± 2 km, although the error in the Skylark 1271 was larger than this, because of the problems mentioned earlier.

3. DATA AND RESULTS

Table 1 lists the rocket firings, and associated information, from which successful daytime releases of lithium vapour were made. The trail was observed from both sites in all cases, except for Lorikeet 2013 for which good data were obtained from one site only.

Figure 6 shows photographs, taken during the trial, of the lithium trail on the monitor C.R.O. screen. Figures 5, 7 and 8 give examples of computer reconstruction of data recorded on magnetic tape. As can be seen in figure 6, at early times a coarse and fast scan is used until the operator is sure he has the trail in his field of view. The scan is then made finer, so that accurate data on the position of the trail may be obtained.

On several trials the lithium cannister continued burning over apogee; for example, up and downleg trails can be seen clearly in figure 5. As mentioned earlier, the apogee point is in such cases clearly identifiable.

Figure 9 shows the evolution of the observed trail from one of the sites for trial Cockatoo 3010. The border of the graph is drawn to enclose the field of view of the instrument. It is seen that over the period of observation, generally lasting 15 minutes (by which time all but the dense apogean portion of trail has grown too faint), excellent data on the evolution of the trail were obtained. Even when overall drift of the trail required changing the azimuth and elevation of the scanner mount during the trial in order to keep the trail in the field of view, equally good data were obtained.

Figures 10 through 22 give the final wind profiles for all firings, in hodograph form.

4. COMPARISON OF RESULTS WITH THEORY

All the daytime wind profiles showed counter-clockwise rotation with increasing altitude, which is the common feature of all twilight vapour releases observed at Woomera, with the exception of Lorikeet 2015 whose hodograph was predominantly polarised in the North-South direction. The classical Hough function for the diurnal (1, -2) mode shows just such a behaviour at 30^{o} latitude, i.e. the East-West component vanishes, and suggests that on this occasion this mode was completely dominant. However, it cannot be as simple as that, because the observed wind profile changes from Northward to Southward at 135 km, which the (1, -2) mode does not.

Forbes and Garret(ref.4) have calculated the solar diurnal tidal structure in the thermosphere. By comparing the latitudinal variation of the wind at different altitudes with the classical Hough modes, they found that the (1,1) mode was dominant up to about 110 km altitude, but that the (1, -2) mode became dominant above that altitude. This is consistent with the observed behaviour of L2015; also, as will be discussed later, the presence of the (1,1) mode is in keeping with the observed data from the other firings.

For all of the other profiles, which do not show such an idiosyncratic behaviour, no clear identification with any particular mode may be made. The commonly observed anti-clockwise rotation of the wind vector with increasing height, with a vertical wavelength greater than 30 km is attributed to a combination of the solar semidiurnal (2,2), (2,4) and, to a lesser extent (2,3) modes. As Hong and Lindzen(ref.5), who developed a three dimensional model of the solar semidiurnal tide, have shown, minor changes in any one of these modes can make gross differences in the final profile. The mode strengths in turn depend critically on the mean winds, especially below 150 km altitude. It is partly for this reason that it is difficult to compare our data with their predictions. It is also because Hong and Lindzen's model at 30^{o} latitude gives very low velocities at 100 km which increase without much change in phase to about

70 ms^{-1} at 120 km, at which altitude the characteristic counter-clockwise rotation of the slowly changing velocity vector starts to occur. The bulk of our results lie in the range 100 to 120 km altitude and already show the developed spiral at these altitudes. Almost certainly this behaviour in our data is due to contribution from the solar diurnal (1,1) mode which, unlike the (1, -2) mode at these altitudes, is not plane polarised.

The only firings for which we have data at higher altitudes is SL1207 (figure 13) and SL1271 (figure 19), which were fired at the same time and season, although two years separated them. In view of the variability of the upper atmospheric tides and other wind components, there is a remarkable similarity between the profiles. Both have a southward velocity at 100 km, rotating counter-clockwise and becoming Westward at 130 km altitude. Interestingly enough, the model of Hong and Lindzen also predicts that the maximum Westward velocity at 130 km will be at about 1100 hr. The profile for SL1271 continues to follow the model above these altitudes, but that for SL1207 appears to be perturbed in the North-South direction. The nature of this perturbation suggests it is due to contributions from the solar diurnal (1, -2) mode.

The rockets C3010, L2011 and L2013 were fired at approximately two hour intervals. A comparison of the observed wind profiles shows them to be remarkably similar in shape, but displaced successively in altitude (figures 14, 16, 18). Because the phase of the tidal modes descend in altitude with time, it would be expected that, if one mode dominates a given wind profile, an orderly descent in the profile with time would be observed. However, the structure of these three profiles, especially the cusp which appears at 112 km on C3010, suggests that no single mode dominates, but yet the three profiles maintain very similar shape as the waves descend. Since the modes which combine to form the profile have different vertical phase velocity, it leads one to expect a change in profile with time. We have no explanation for this contradiction between expected behaviour and the observations, other than to suggest it may be a non-linear "lock-in" of the modes.

5. WIND INDUCED IONOSPHERIC EFFECTS

During the latter part of the period over which the firings were made, an ionosonde and magnetometer were operational at the B5 site. Both instruments gave data for the weeks starting 22 February, 24 May and 28 June, 1976. There were no magnetic storms recorded for at least 24 hours before any of the firings; the sum of the 3-hourly Kp magnetic index for the previous 24 hours being 9, 12 and 10 respectively. However, the ionograms showed T.I.D. (travelling ionospheric disturbance) activity for 24 February 1976. This was especially strong from 0800 to 0900 C.S.T. Figure 23 is a tracing off the ionograms for this period. Note that, contrary to what frequently occurs, these T.I.D.s did not give rise to sporadic E layers.

A more general mechanism for the formation of sporadic E layers, is that of a vertical shear in the horizontal wind (Whitehead(ref.6)). There is substantial evidence that temperate zone sporadic E layers are produced by metal ions, deposited by meteors, which have been concentrated into layers by the dynamo action of the horizontal neutral wind across the earth's magnetic field (see, for example, Narcisi(ref.7)). The layers form where the vertical ion motion decreases through zero with increasing altitude. We have calculated the vertical ion motion, v_z, using the expression

$$v_z = \frac{\rho}{1+\rho^2} \cdot \Gamma_y \cdot u_x + \frac{1}{1+\rho^2} \cdot \Gamma_y \Gamma_z u_y$$

where

ρ = ratio of collision-frequency to gyro-frequency for ions

Γ_y, Γ_z = cosine and sine of angle of magnetic dip

u_x, u_y = horizontal component of neutral wind, in magnetic Eastward and Northward directions.

We have had to neglect the contribution of the ambient electric field as it is not known. However, this contribution is not greater than 10%.

In figure 15, 17, 20, 22, are plotted the vertical ion velocities of the trials for which there were ionograms recorded: C3010, L2011, SL1271 and L2015 respectively. All the profiles had a zero crossing with increasing altitude in the sense required to produce ion convergence, the respective altitudes being 121, 95, 123 and 134 km. Despite this favorable condition for sporadic E, with the exception of two weak layers (and some very strange layers produced by the release which will be discussed in another report), no sporadic E was produced. The exceptions were a weak cusp Es layer at 120 km, at around the time at which C3010 was fired, and a broad, broken, and variable layer lying between 120 and 130 km from an hour before the time of launching of SL1271, until just before launching time. The heights of these layers agree with the predictions of the wind shear theory, but their weakness, and the absence of any sporadic E on the other occasions, indicate that favorable wind shears are not a sufficient condition for Es, but that the presence of metal ions in the appropriate region is also necessary.

6. SUMMARY

This collection of data on wind profiles in daytime, shows similar structure and variations as have been previously observed at twilight. Particular points that come out of the observations were:

(a) In one case the velocity profile was polarised in the North-South direction. This behaviour is predicted for the solar diurnal tide (1, -2) mode, which suggests that this mode was the dominant contribution to the observed wind profile.

(b) In most of the other cases the major contribution to the observed wind profiles appeared to be the solar semidiurnal tide above 120 km, and the solar diurnal (1, 1) mode below that altitude.

(c) The two Skylark trials were fired at the same time of day and season, albeit in different years. They gave data with remarkable similarity, which agreed well with the predicted solar semidiurnal tide.

(d) Although, in every case examined, the form of the wind profile was favorable for the formation of sporadic E, on only two occasions was Es observed, and then only very weakly. The winds are therefore only a necessary, but not a sufficient condition for Es formation; it being often the case that the metal ion concentration is not great enough to give an observed layer.

ACKNOWLEDGEMENTS

The Cockatoo and Lorikeet vehicles were fired as part of the Australian Defence Scientific Services Upper Atmosphere Research program. Preparation and launch of the vehicles was undertaken at Weapons Research Establishment under the

direction of Mr. R. Bissell. The Skylark rocket formed part of the British Space Research program, and we are grateful to Dr. D. Rees, University College London, for his invitation to participate in the observations.

We wish to thank Messrs. C. Beach, W. Horne, and N. Talkington of Weapons Research Establishment for their assistance in maintaining the daylight scanners and obtaining the data.

REFERENCES

No.	Author	Title
1	Bedinger, J. Manring, E. and Ghosh, H.	"Study of Sodium Vapour Ejected into the Upper Atmosphere". J. Geophys. Res. 63, 19, 1958
2	Hind, A.D. and Lloyd, K.H.	"A Field of View Scanning Photometer to Detect Weak Emissions against a Bright Sky Foreground". WRE-TM-1021 (WR&D), 1973
3	Hind, A.D. and Lloyd, K.H.	"A Determination of the daytime thermospheric Wind Profile by Observing a Lithium Trail with a Field of View Scanner". Aust. J. Phys. 27, 401, 1974
4	Forbes, J.M. and Garrett, H.B.	"Solar Diurnal Tide in the Thermosphere". J. Atmos. Sci. 33, 2226, 1976
5	Hong, S. and Lindzen, R.S.	"Solar Semidiurnal Tide in the Thermosphere". J. Atmos. Sci. 33, 135, 1976
6	Whitehead, J.D.	"The Formation of Sporadic E Layers in Temperate Zones". J. Atmos. Terr. Phys. 20, 49, 1961
7	Narcisi, R.	"Metal ion Layers in the E Region". Space Research VIII, p 360, Ed. A. Mitra, L. Jacchia and W. Newman. North Holland Pub. Co., 1968

TABLE 1. DAYTIME LITHIUM RELEASES AT WOOMERA

Vehicle	Date	C.S.T.	U.T.
Cockatoo 2004	21 June 1973	08 50 00	23 20 00
Cockatoo 2001	19 September 1973	14 30 00	05 00 00
Cockatoo 3004	19 March 1974	12 28 00	02 58 00
Skylark 1207	23 April 1974	10 33 00	01 03 00
Cockatoo 3010	24 February 1976	07 00 00	21 30 00
Lorikeet 2011	24 February 1976	09 00 00	23 30 00
Lorikeet 2013	24 February 1976	12 00 00	02 30 00
Skylark 1271	27 May 1976	10 00 00	00 30 00
Lorikeet 2015	30 June 1976	10 00 00	00 30 00

APPENDIX I. ANGULAR CALIBRATION OF DAYTIME LITHIUM SCANNER USING THE SUN

SUN CAL 89 SL1271 MAY 76 0. 0. 0. 551.00 30.00 0 0 2

SCAN SITE	LATITUDE	LONGITUDE	UT DATE	SID TIME	RIGHT ASCENSION		DECLINATION		LAT RANGEHEAD LONG	
	-31 3 58	-135 52 23	27 MAY1976	16 18 42	4 15 45	4 19 48	21 16 48	21 26 41	-30 56 40	-136 31 19

SCANNER MOUNT CORRECTIONS AZ= 60 0 0 EL= 0 10 0 SCAN MOUNT READING FOR ZERO EL OF OPTIC AXIS 40 4 0
SITE TO RANGEHEAD ORIENT. A= 282.506 E= 0.569 P= 282.172 N.B. ALL AZIMUTHS ARE WEST OF NORTH

FRME NO.	POIN NO.	TRUE SUNS-AZ	TRUE SUNS-EL	READ X-VOLTAGE	CALC XALPHA-AN	READ Y-VOLTAGE	CALC YALPHA-AN	TRUE CORRECTED AZ-SCANR-OP-AXIS-EL		U.T.(HRS)	READ OFF MOUNT AZ-SCAN-OP-AXIS-EL	
2	2	340.379	35.118	-359.000	-5.686	658.000	12.819	353.973	10.001	1 44 59	354.000	50.000
3	3	340.926	35.260	-101.000	-16.872	610.000	15.106	21.982	10.065	1 47 0	22.000	50.000
4	4	341.997	35.527	-100.000	-17.233	380.000	22.384	22.011	-5.935	1 50 55	22.000	34.000
5	5	342.804	35.716	-378.000	-4.931	348.000	22.718	354.026	-9.499	1 53 51	354.000	30.500
6	6	343.626	35.899	-639.000	6.841	329.000	22.950	328.028	-9.572	1 56 49	328.000	30.500
7	7	344.984	36.181	-656.000	7.513	277.000	24.852	328.039	-13.072	2 1 41	328.000	27.000
8	8	345.836	36.344	-369.000	-5.425	275.000	25.279	358.037	-13.988	2 4 43	358.000	25.000
10	10	347.991	36.712	-134.000	-15.610	522.000	17.786	25.992	5.071	2 12 19	26.000	45.000
11	11	348.829	36.838	-366.000	-5.530	494.000	18.116	1.998	1.022	2 15 15	2.000	41.000
12	12	349.791	36.970	-670.000	8.288	472.000	18.491	329.997	0.933	2 18 36	330.000	41.000
13	13	350.925	37.111	-560.000	3.037	266.000	25.356	344.039	-13.526	2 22 32	344.000	26.500
114	114	352.098	37.238	-542.000	2.543	512.000	17.176	345.992	2.979	2 26 35	345.000	43.000

LEAST SQUARES FIT VOLTS TO ANGLE CONVERSION
ALX = -0.38378 + -0.00078 VX + 0.00001 VY
ALY = 0.60936 + 0.00003 VX + -0.00057 VY

SUN'S AZ. AND EL. FRAME-NO	POINT-NO	MIRROR ANGLE DEG X FROM LST	SOU Y	WITH RESPECT TO SCANNER SITE PLANE DATA-AZ	CALC-AZ	DATA-EL	CALC-EL	WITH RESPECT TO RANGEHEAD PLANE TRUE AZ	CALC AZ	TRUE EL	CALC EL	ANGLE DIFF.
114	2	-5.528	12.896	340.379	340.732	35.118	35.298	341.056	341.412	35.416	35.594	0.340
114	3	-17.058	14.933	340.926	340.648	35.260	34.862	341.607	341.323	35.554	35.158	0.459
114	4	-17.265	22.398	341.997	341.917	35.527	35.540	342.685	342.605	35.811	35.825	0.066
114	5	-4.901	22.920	342.804	342.833	35.716	36.119	343.497	343.532	35.994	36.396	0.403
114	6	6.715	23.051	343.626	343.367	35.899	36.113	344.324	344.068	36.170	36.386	0.299
114	7	7.435	24.707	344.984	344.768	36.181	35.906	345.691	345.470	36.439	36.167	0.325
114	8	-5.353	25.305	345.836	345.992	36.344	36.402	346.548	346.705	36.595	36.651	0.138
114	10	-15.650	17.727	347.991	347.946	36.712	36.589	348.715	348.668	36.943	36.821	0.127
114	11	-5.332	18.205	348.829	349.274	36.838	37.042	349.557	350.006	37.061	37.262	0.410
114	12	8.197	18.354	349.791	349.522	36.970	36.724	350.523	350.251	37.185	36.942	0.326
114	13	3.150	25.242	350.925	351.167	37.111	36.879	351.663	351.902	37.315	37.081	0.302
114	114	2.522	17.294	352.098	352.064	37.238	37.474	352.841	352.810	37.432	37.668	0.237

CAL. REF. VOLTS = 551.00 30.00 DATA REF. VOLTS = 551.00 30.00

BEST AVAILABLE COPY

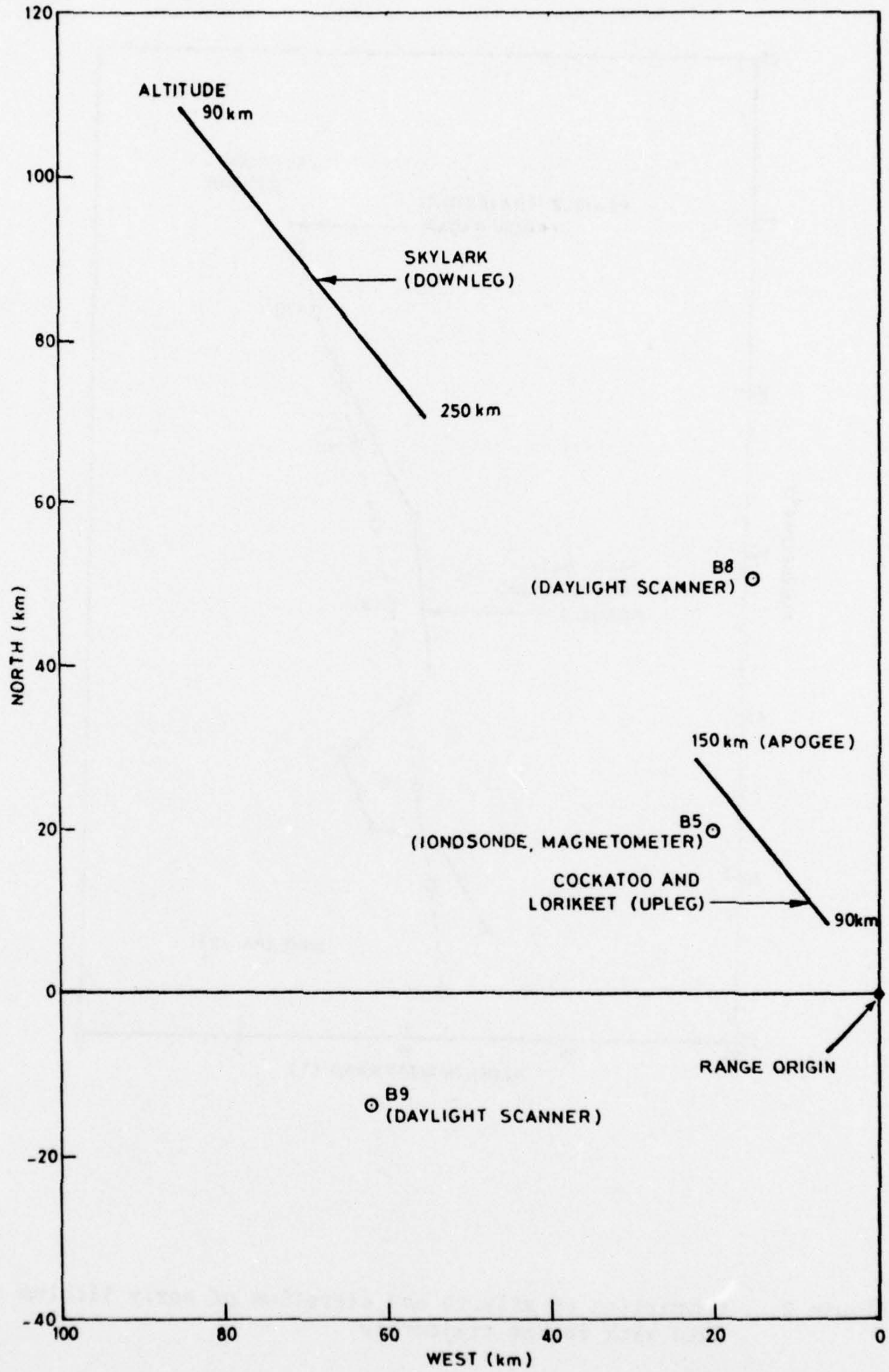

Figure 1. Disposition of sites and typical rocket trajectories

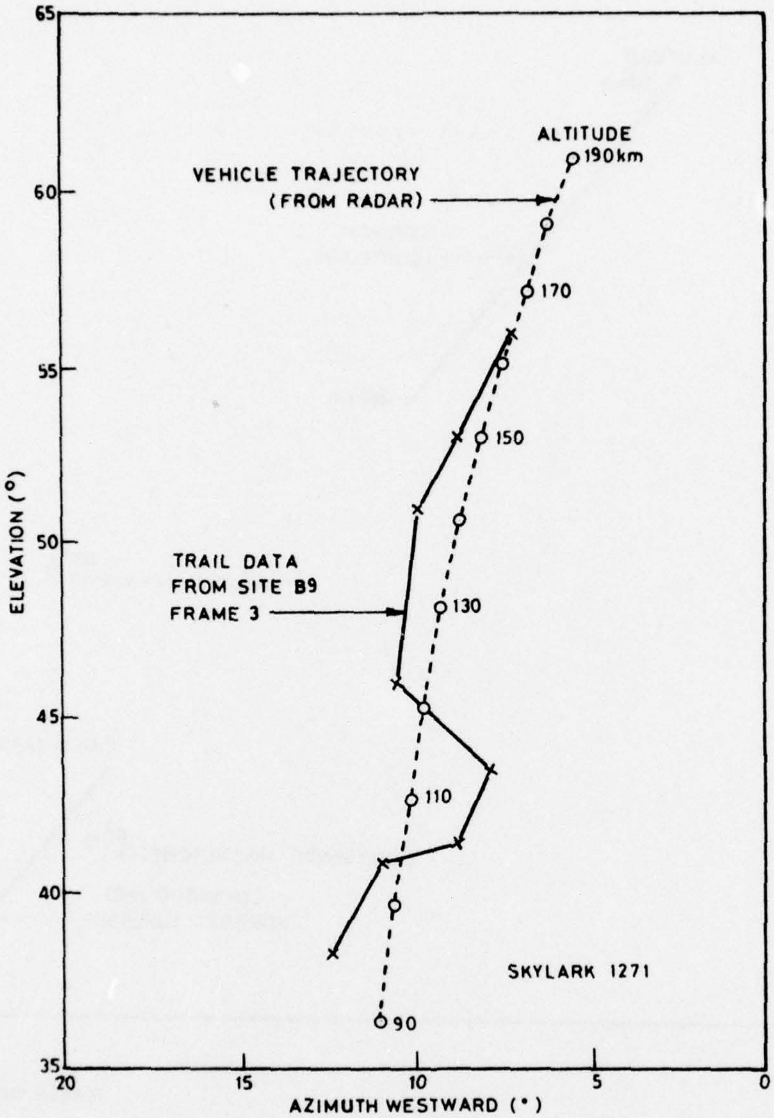

Figure 2. Comparison of azimuth and elevation of early lithium trail data with rocket trajectory

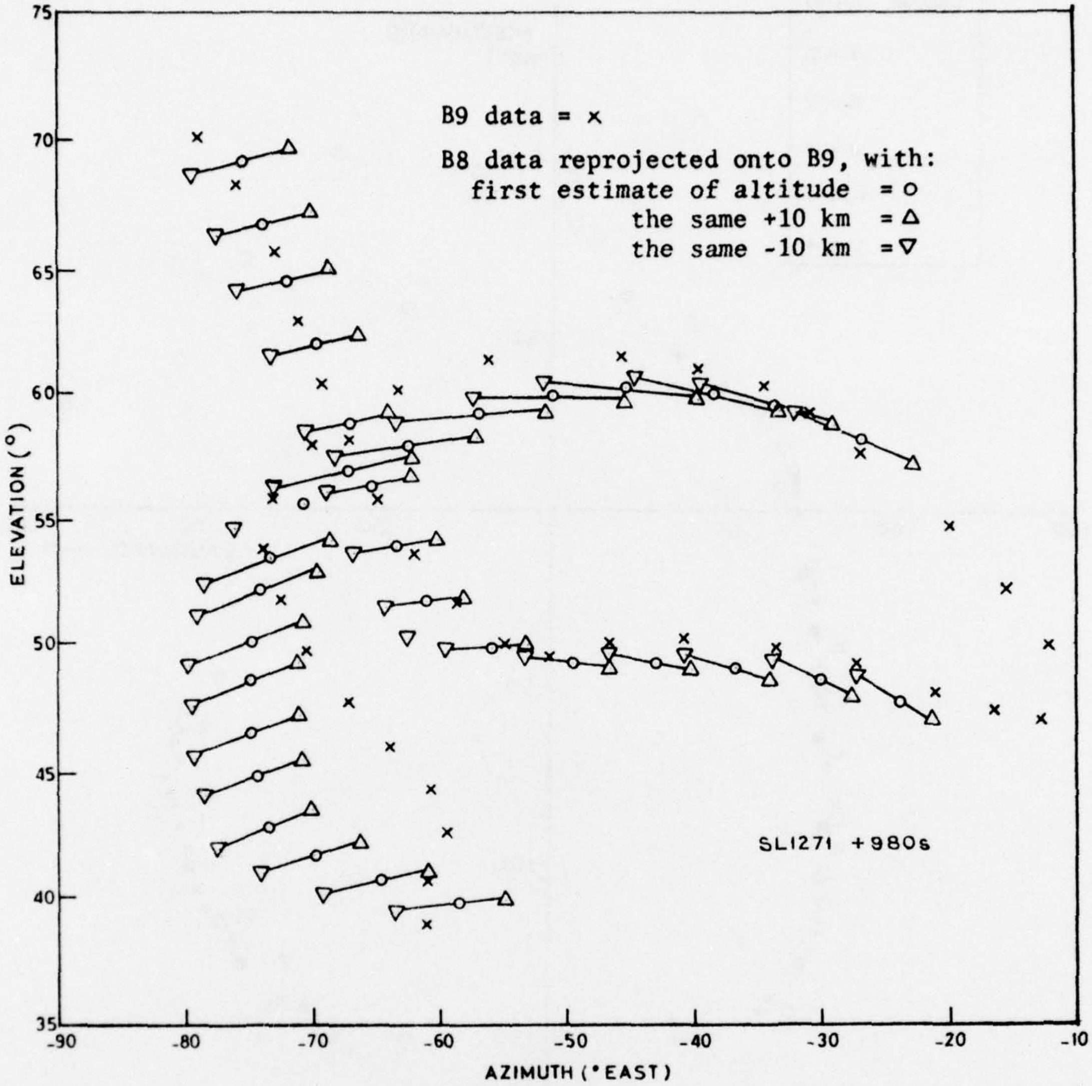

Figure 3. Comparison of observed data with reprojected data from other site using method of assigned altitudes

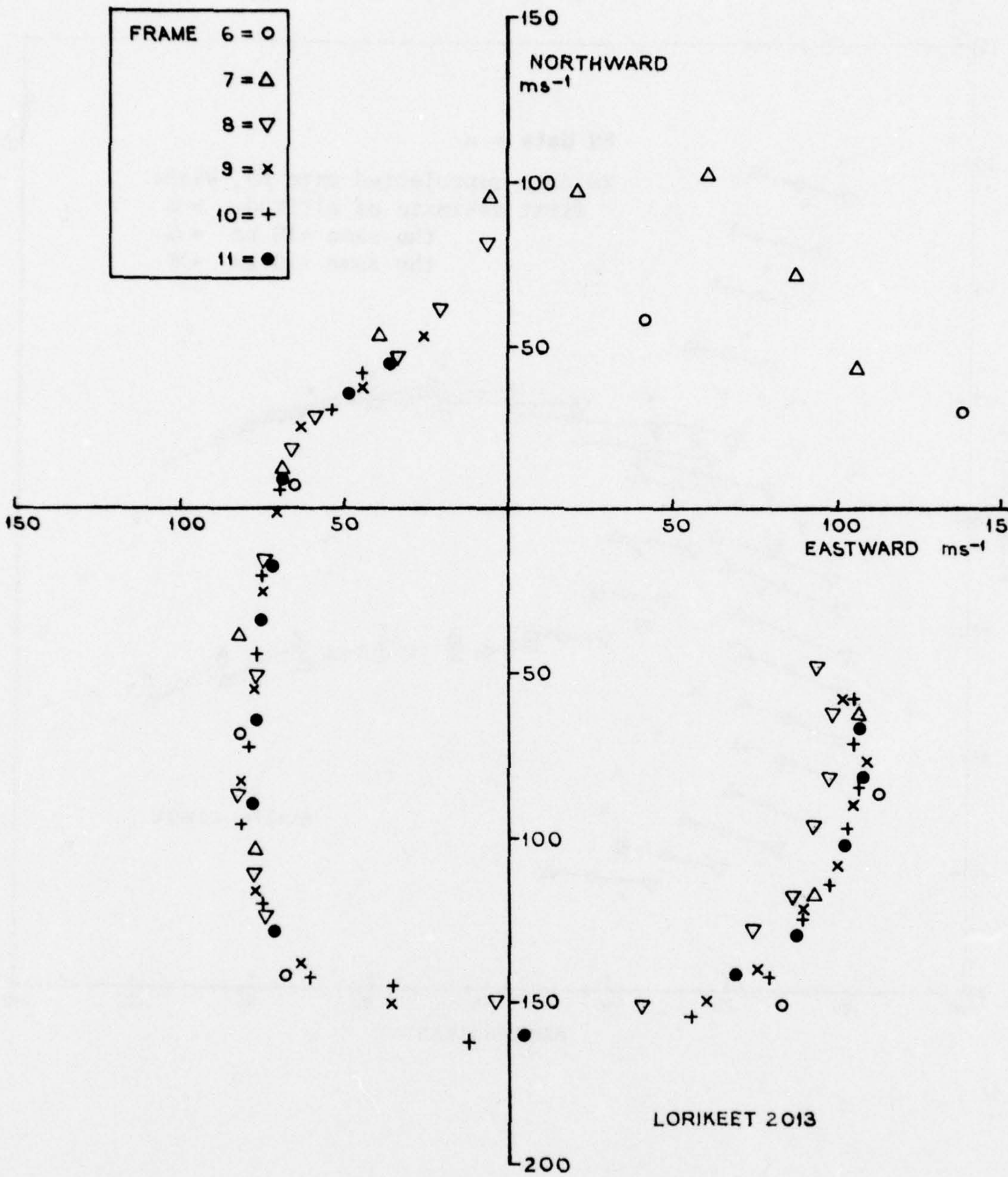

Figure 4. Wind hodograph calculated from data from site B8

BEST AVAILABLE COPY

TRIAL APS/V SITE 66 FRAME NO. 6 DATA TYPE ACT.D

START T 328.6 END T 349.2 NO. OF SCAN LINES 32 DIGITISATION RATE 100 PER SEC. MAX U MIN SIGNAL 30.000 4.000
EACH DATA POINT IS SHIFTED BY 2 MATRIX CELLS
CONTOURS AT 4.03 - 7.74 + 11.45 * 15.17 $ 18.88 I 22.60 X 26.31 S 30.00

FLAG SHOWED PERMANENT REDUNDANCIES = 0

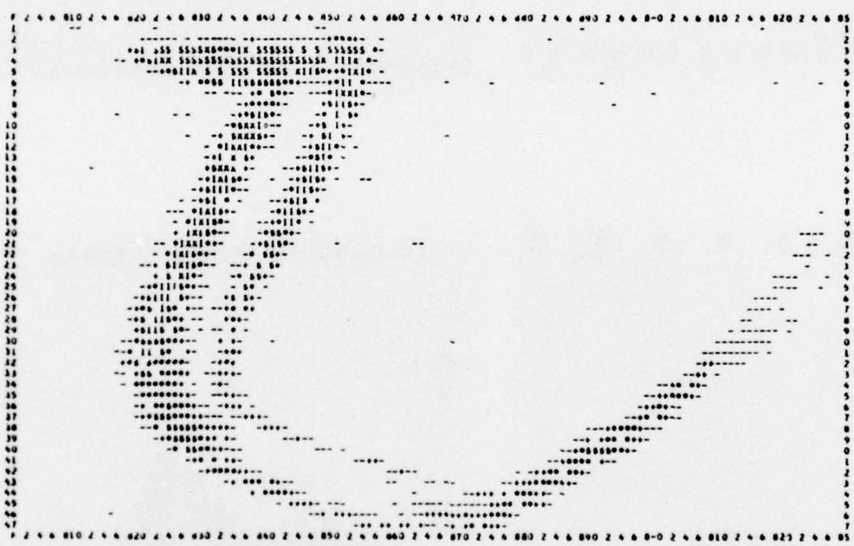

TRIAL APS/V SITE 66 FRAME NO. 15 DATA TYPE ACT.D

START T 883.6 END T 950.6 NO. OF SCAN LINES 64 DIGITISATION RATE 100 PER SEC. MAX U MIN SIGNAL 35.000 5.000
EACH DATA POINT IS SHIFTED BY 2 MATRIX CELLS
CONTOURS AT 5.03 - 9.32 + 13.60 * 17.89 $ 22.17 I 26.46 X 30.74 S 35.00

FLAG SHOWED PERMANENT REDUNDANCIES = 0

Note: Release of lithium continued over apogee. These computer plots were generated from magnetic tape data.

Figure 5. Observations of lithium trail from Cockatoo 3004

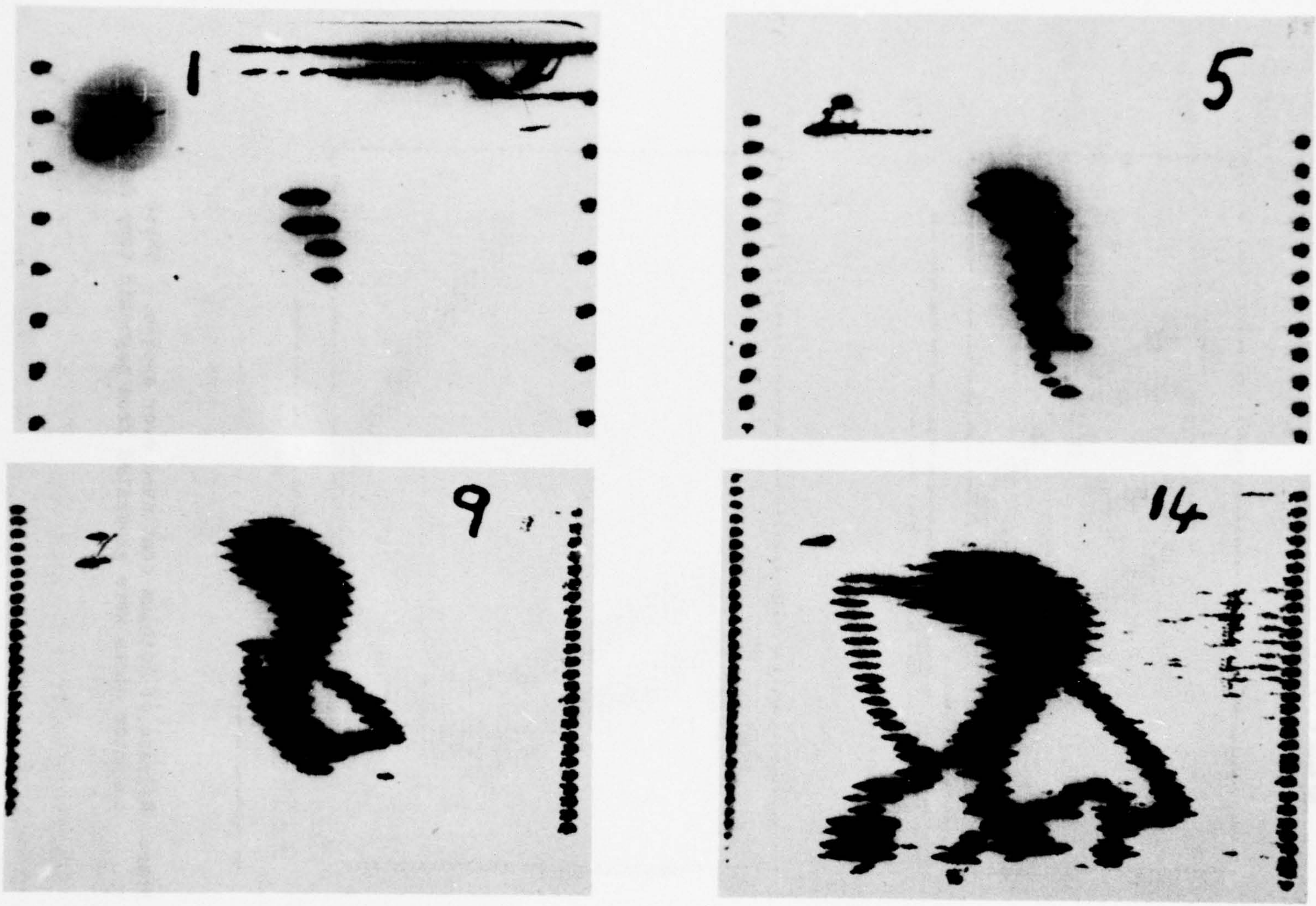

These photographs were taken off the monitor CRO. The perturbation at the bottom of frame 14 is due to cloud.

Figure 6. Observations of lithium trail from skylark 1207

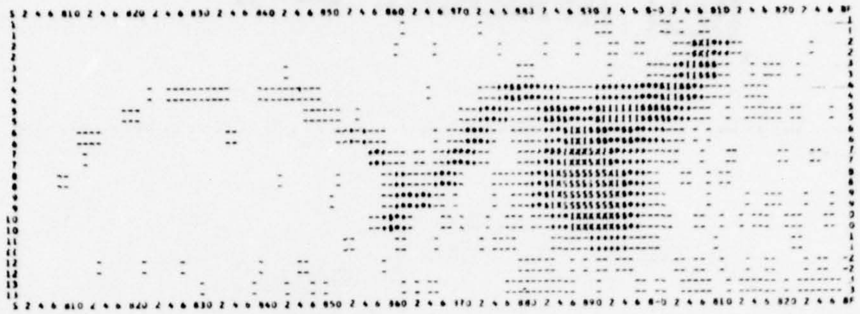

TRIAL A5/15 SITE #8 FRAME NO. 6 DATA TYPE ACT.D

START T 350.2 END T 391.2 NO. OF SCAN LINES 32 DIGITISATION RATE 100 PER SEC. MAX U MIN SIGNAL 50.000 13.333
EACH DATA POINT IS SHIFTED BY 1 MATRIX CELLS
CONTOURS AT 13.34 - 18.58 + 23.82 * 29.07 $ 34.31 I 39.55 X 44.79 S 50.00

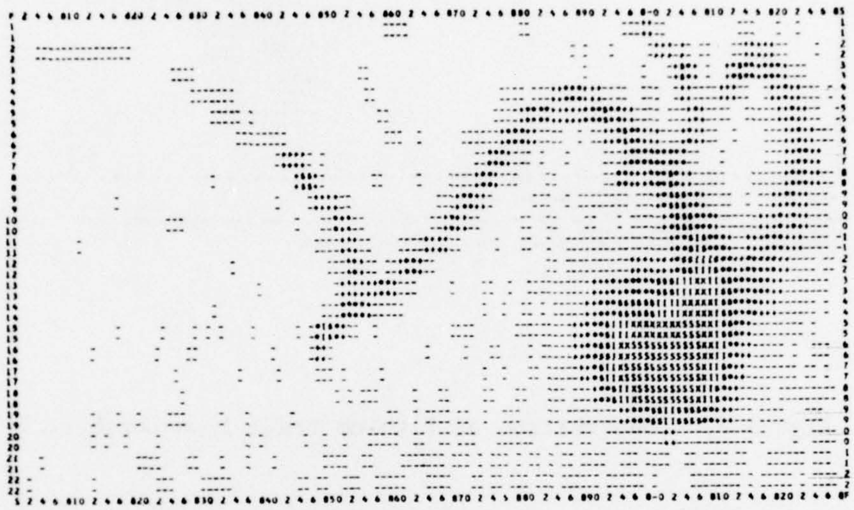

TRIAL A5/15 SITE #8 FRAME NO. 9 DATA TYPE ACT.D

START T 596.5 END T 677.1 NO. OF SCAN LINES 32 DIGITISATION RATE 100 PER SEC. MAX U MIN SIGNAL 45.000 13.800
EACH DATA POINT IS SHIFTED BY 1 MATRIX CELLS
CONTOURS AT 13.83 - 18.29 + 22.75 * 27.20 $ 31.66 I 36.12 X 40.57 S 45.00

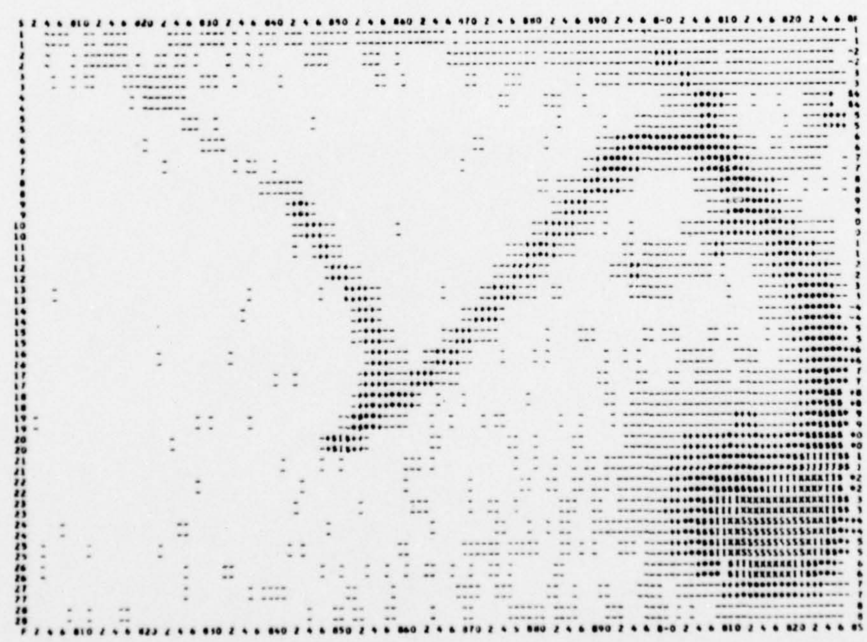

TRIAL A5/15 SITE #8 FRAME NO. 11 DATA TYPE ACT.D

Figure 7. Observations of lithium trail from Cockatoo 3010

BEST AVAILABLE COPY

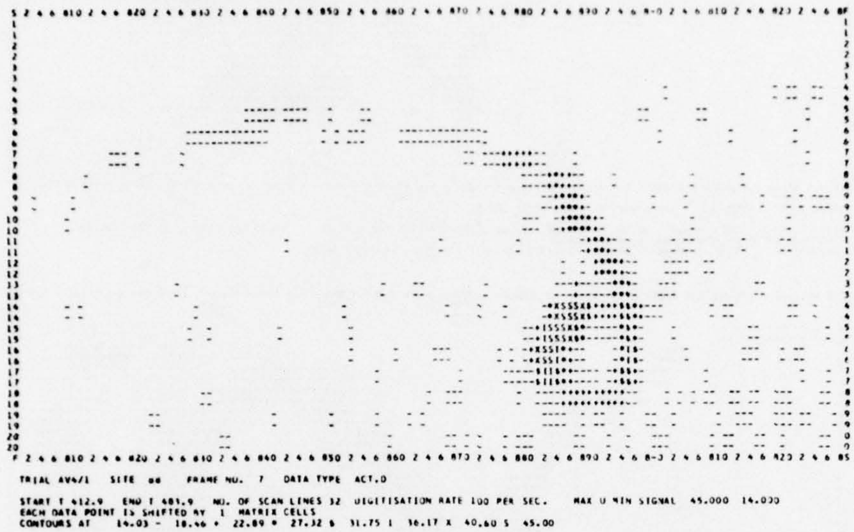

Figure 8. Observation of lithium trail from Lorikeet 2011

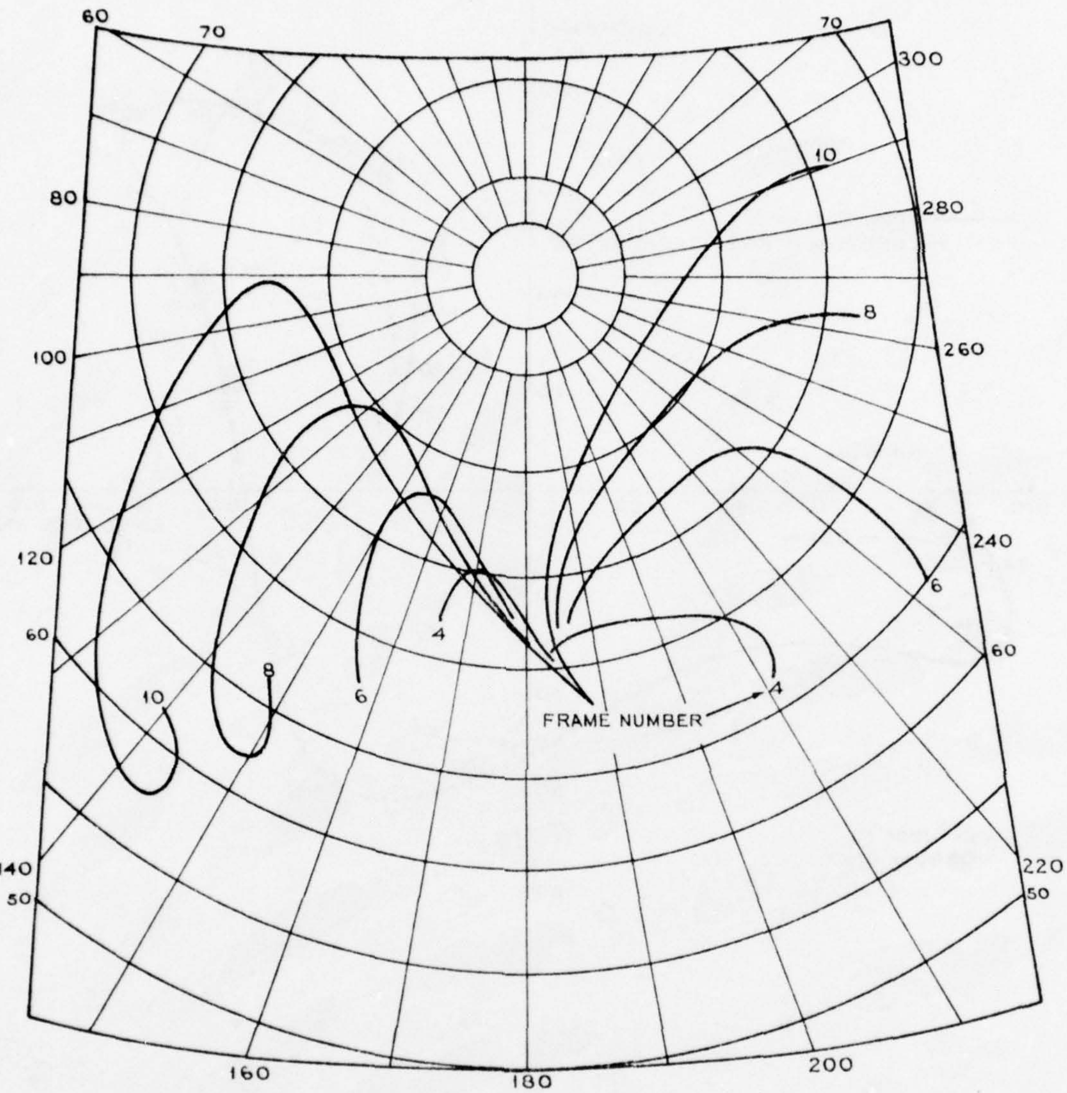

Figure 9. Evolution of trail from Cockatoo 3010 observed from site B8

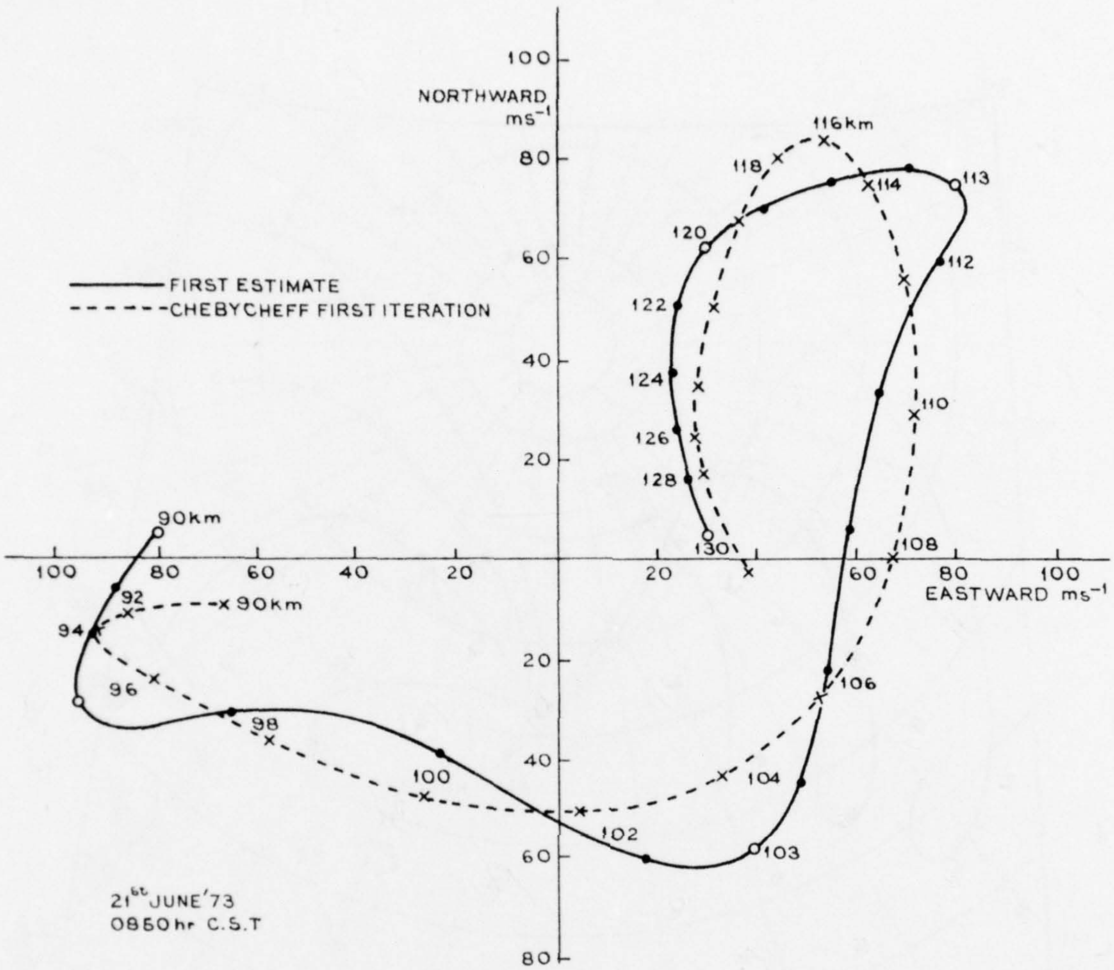

Figure 10. Wind hodograph for Cockatoo 2004

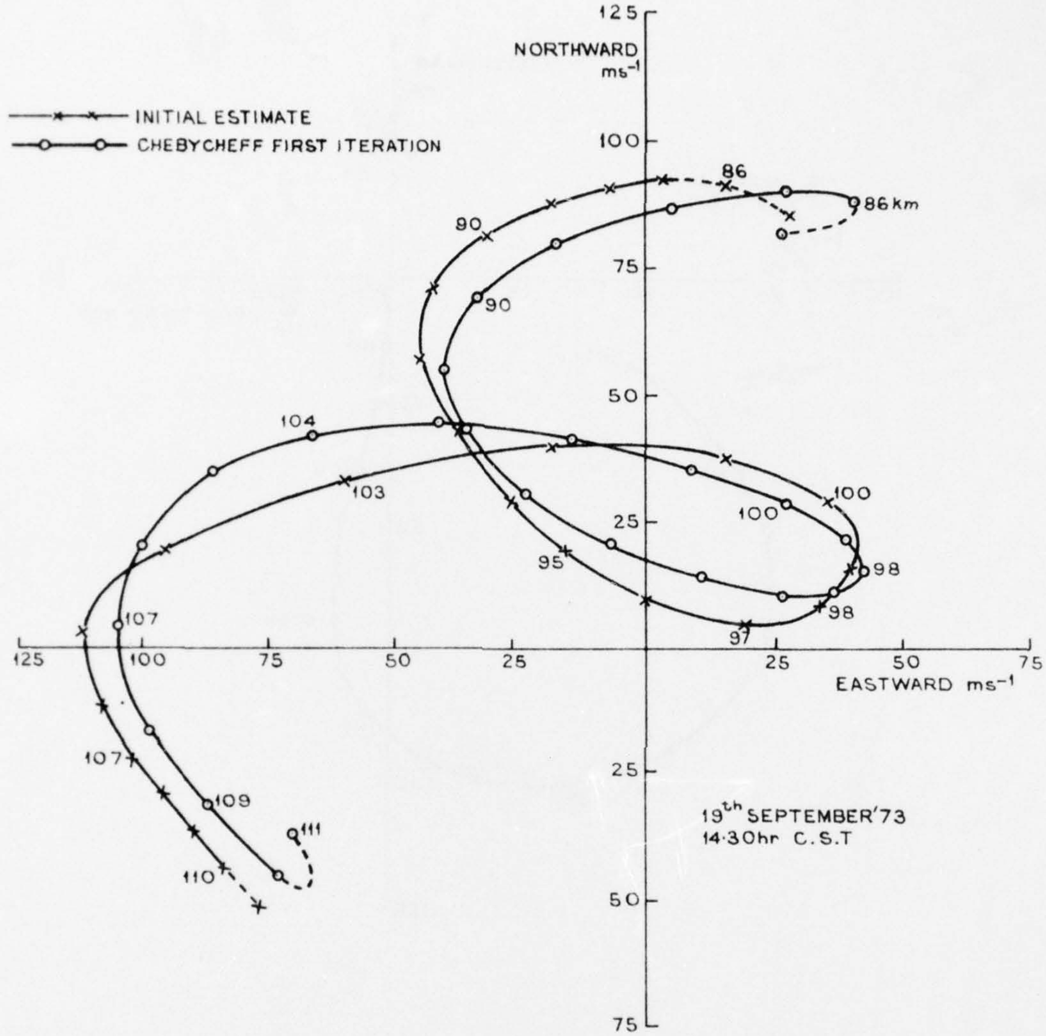

Figure 11. Wind hodograph for Cockatoo 2001

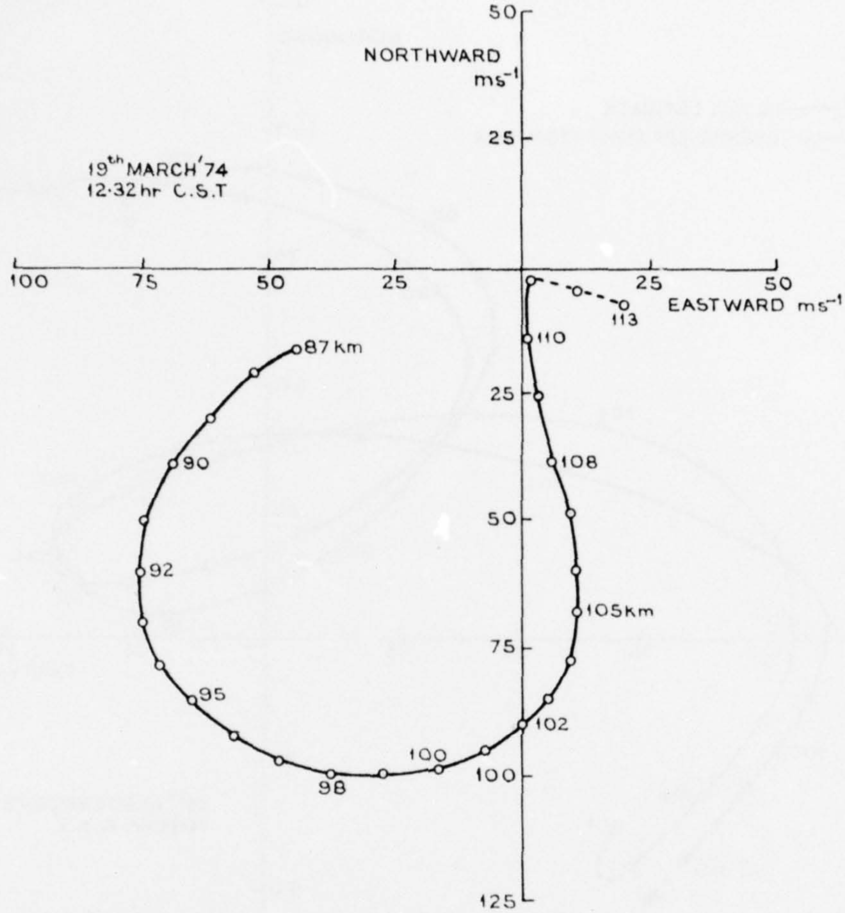

Figure 12. Wind hodograph for Cockatoo 3004

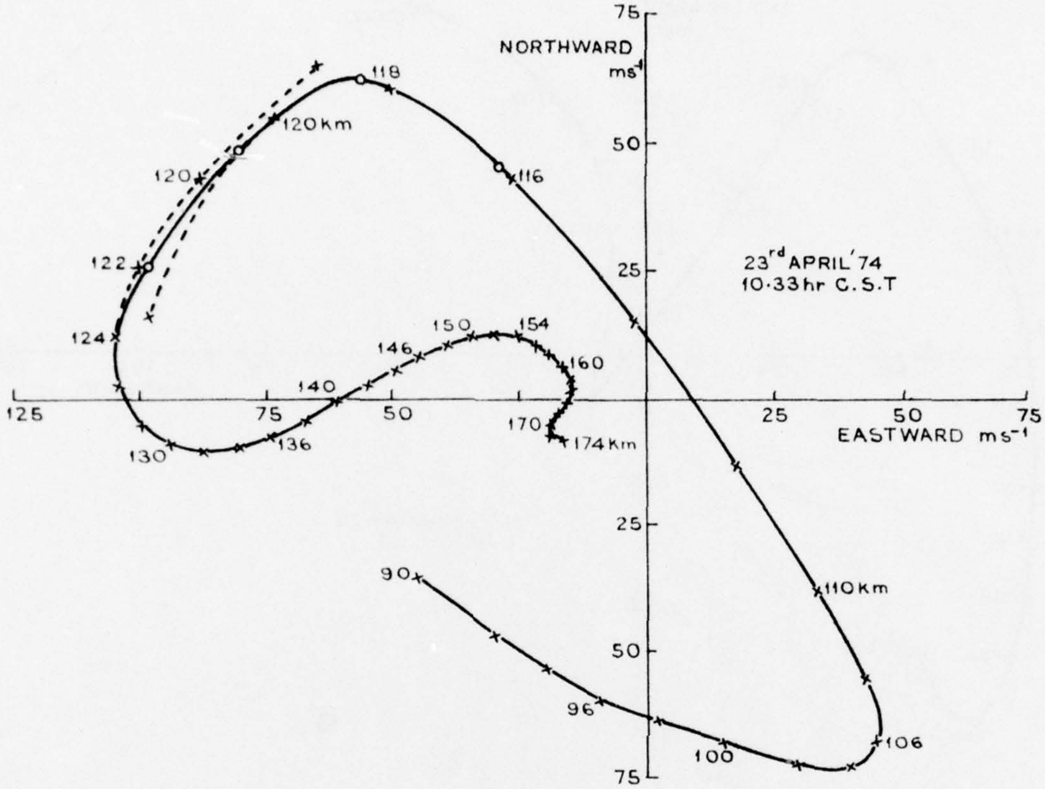

For determining the Chebychev coefficients the profile and the data were separated into two height bands. The connecting points are plotted as circles.

Figure 13. Wind hodograph for Skylark 1207

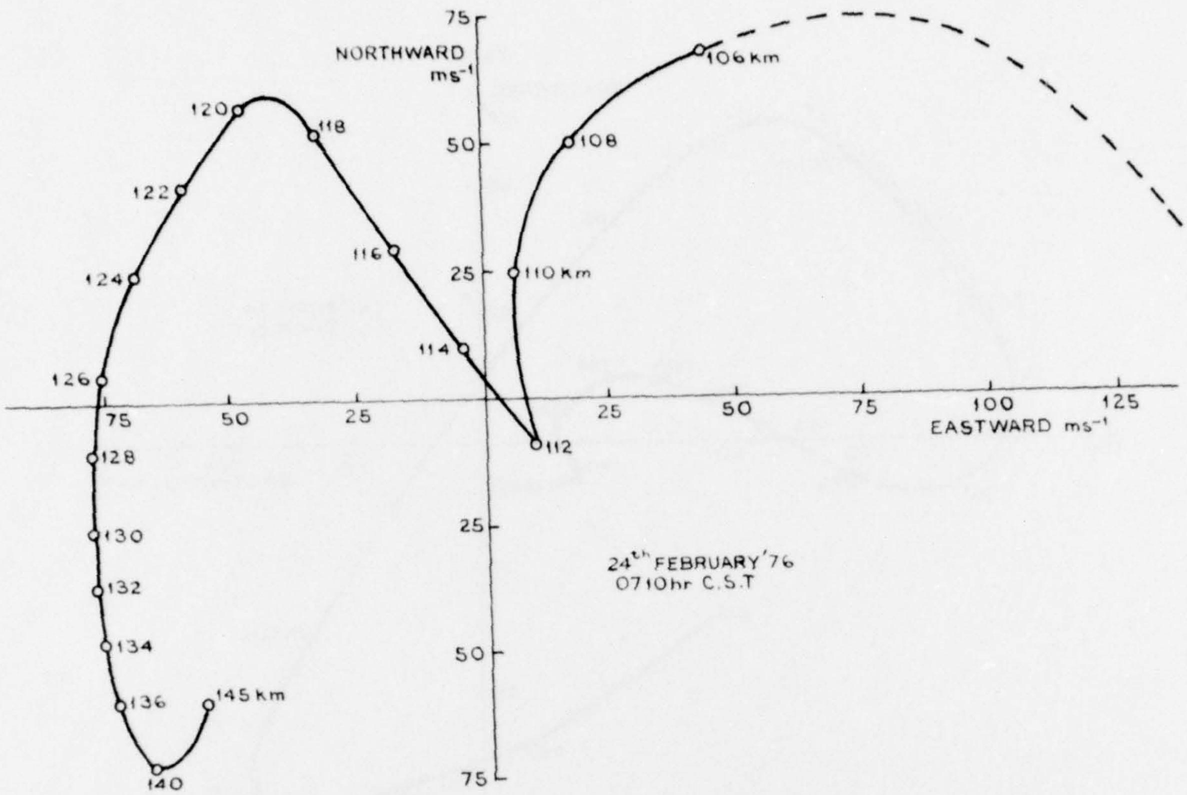

Dashed line indicates data were observed from one site only.

Figure 14. Wind hodograph for Cockatoo 3010

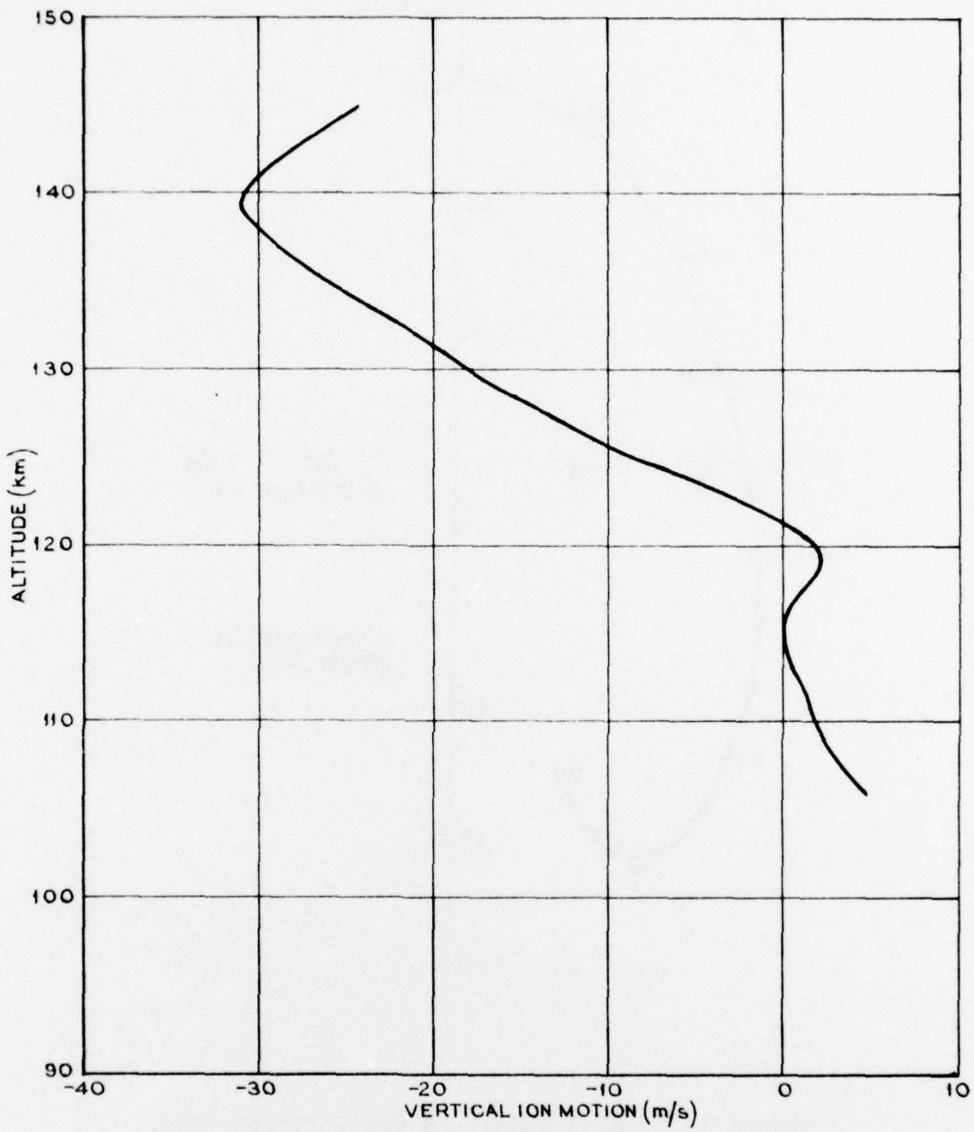

The profile was calculated from the observed neutral wind profile, using the expression given in the text.

Figure 15. Vertical ion motion calculated for Cockatoo 3010

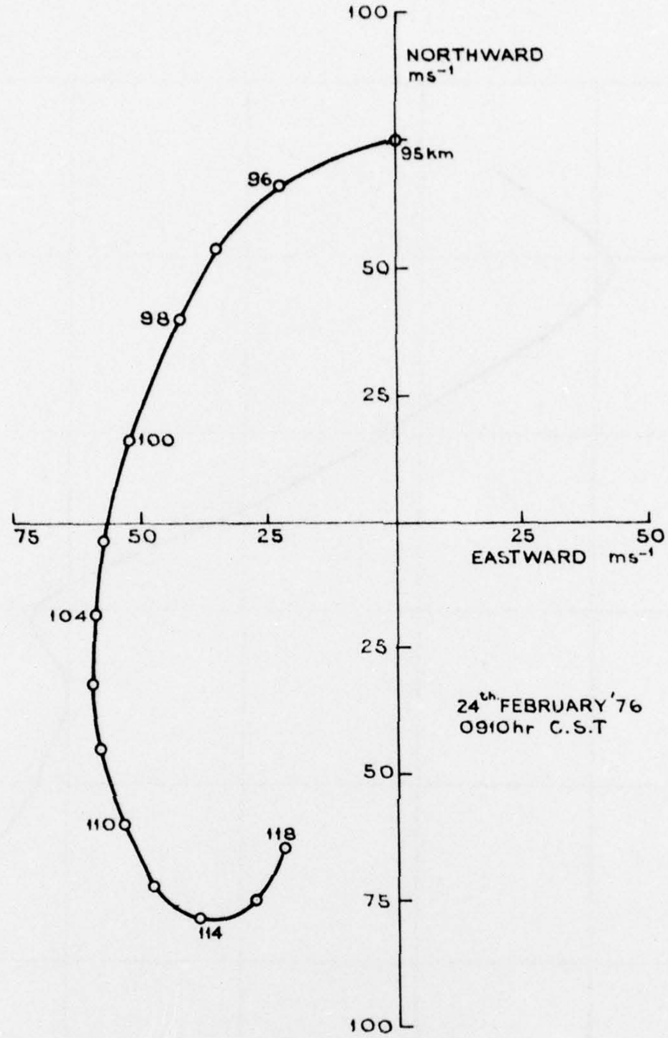

Figure 16. Wind hodograph for Lorikeet 2011

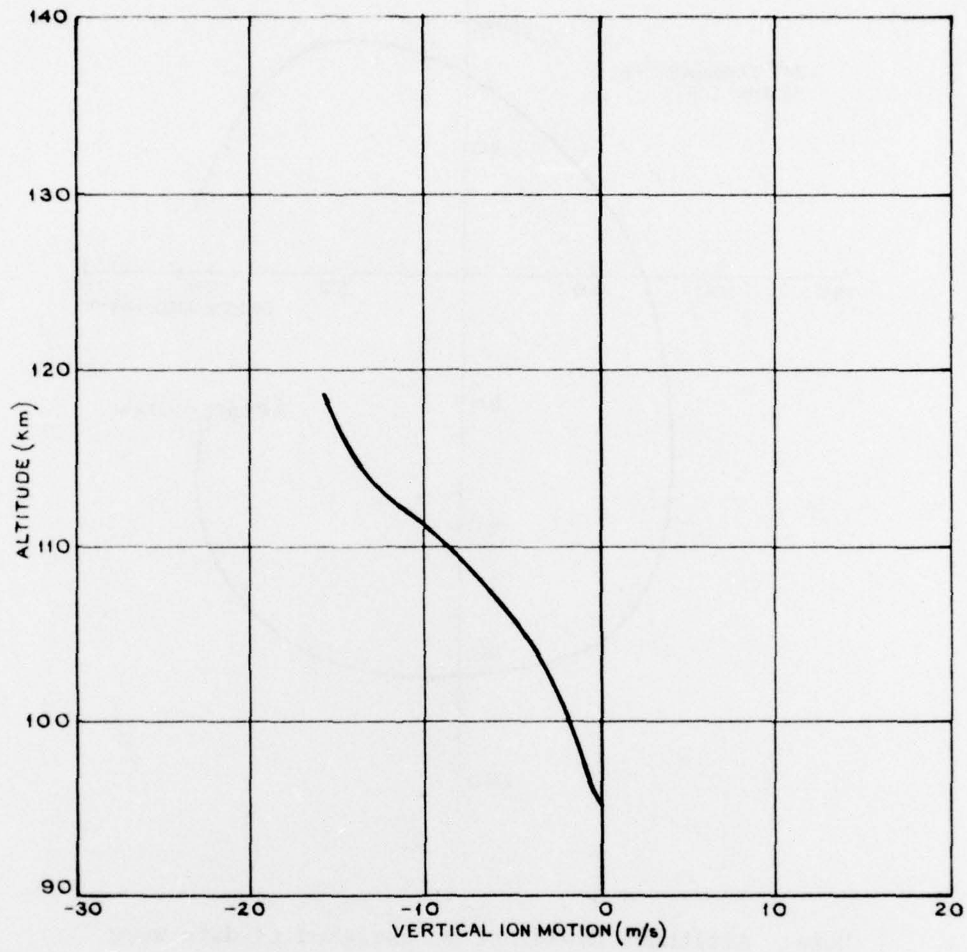

Figure 17. Vertical ion motion calculated for Lorikeet 2011

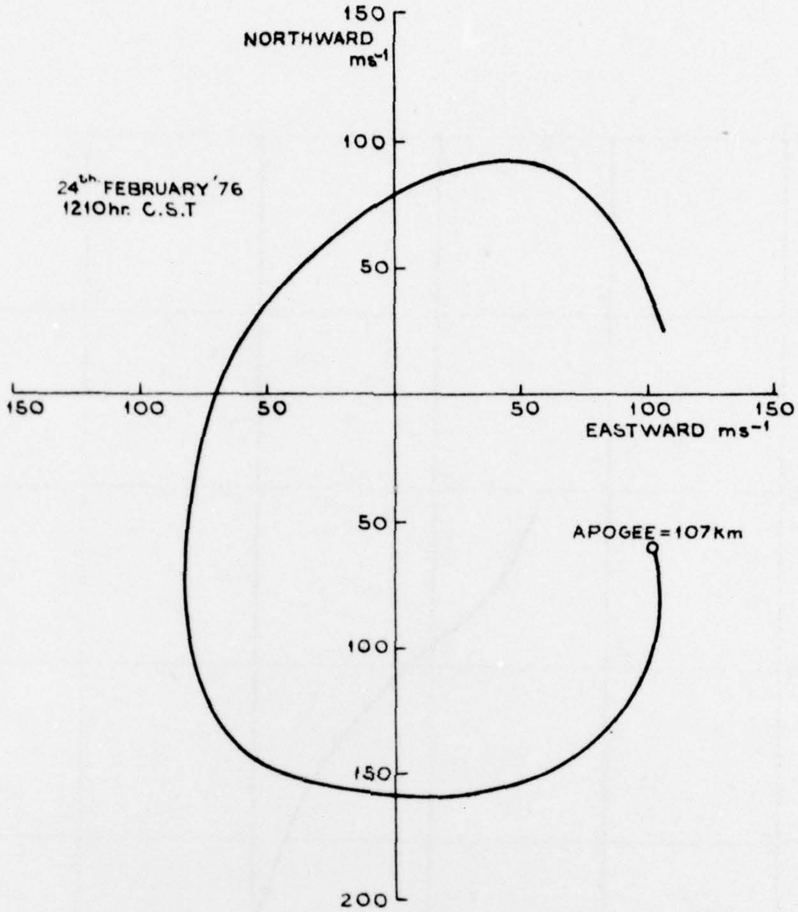

Note: Altitudes could not be assigned as data were obtained only at one site.

Figure 18. Wind hodograph for Lorikeet 2013

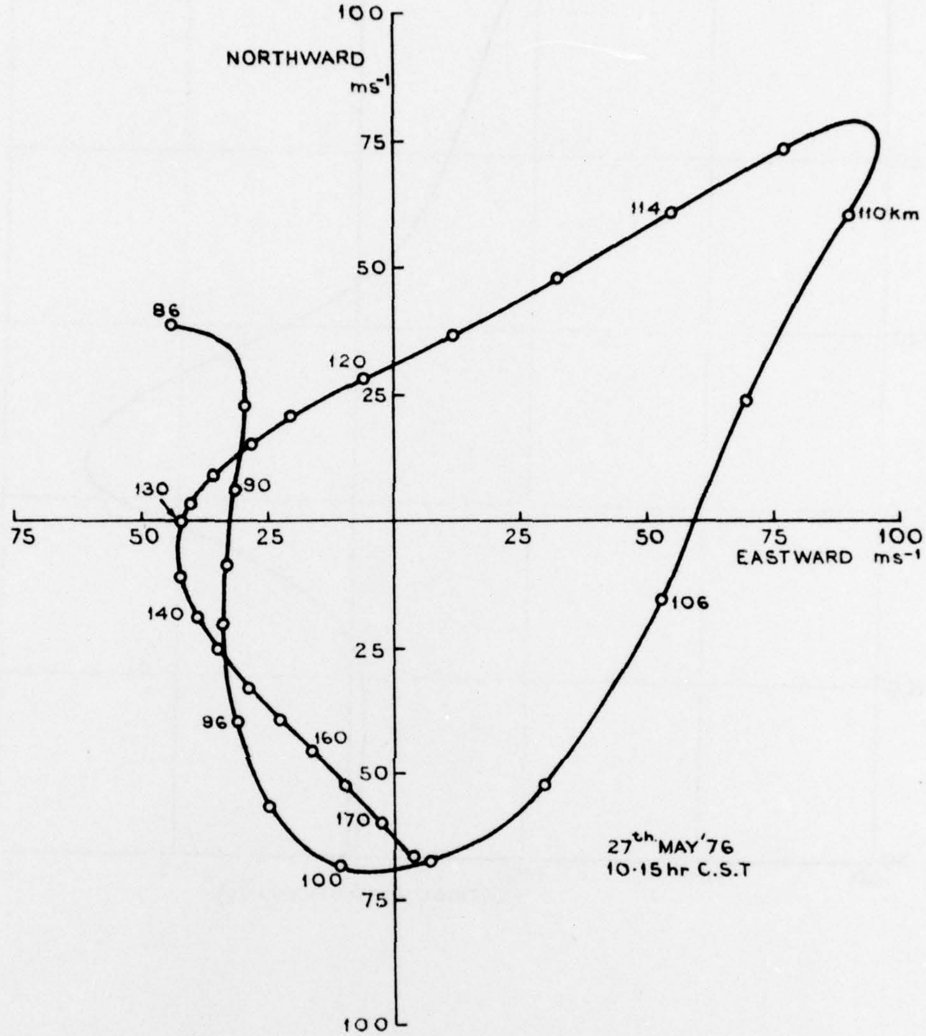

Figure 19. Wind hodograph for Skylark 1271

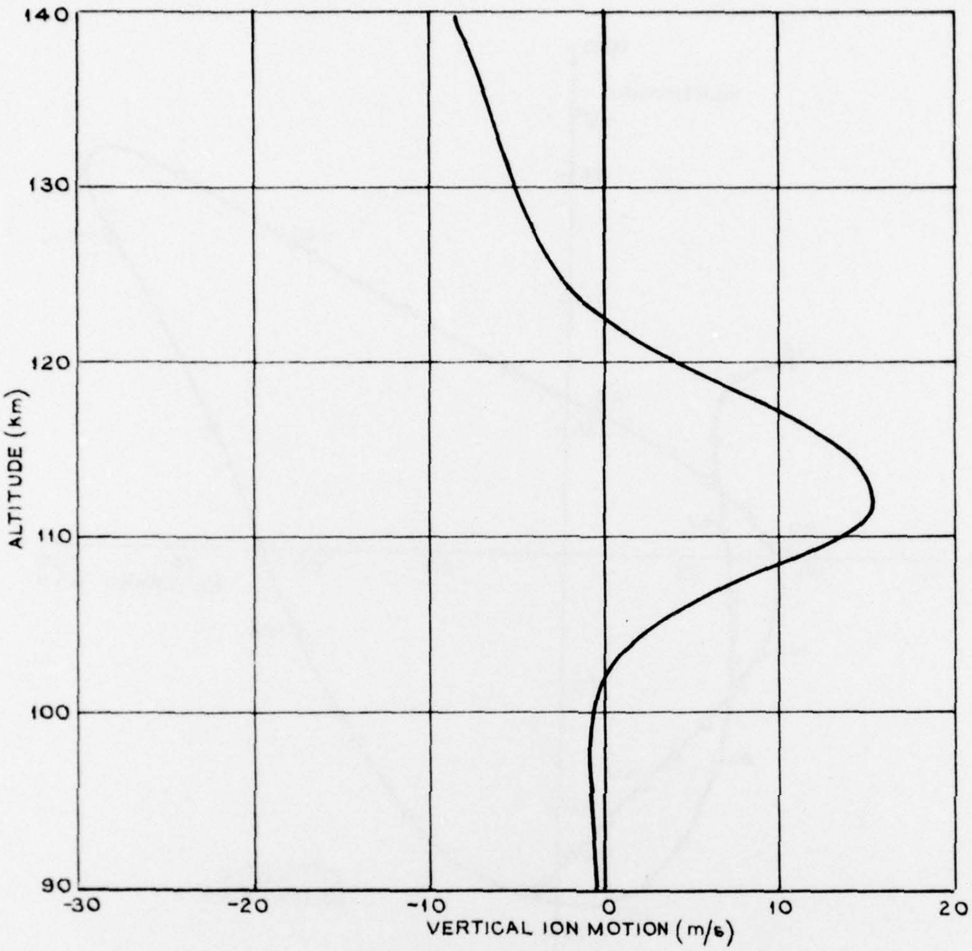

Figure 20. Vertical ion motion calculated for Skylark 1271

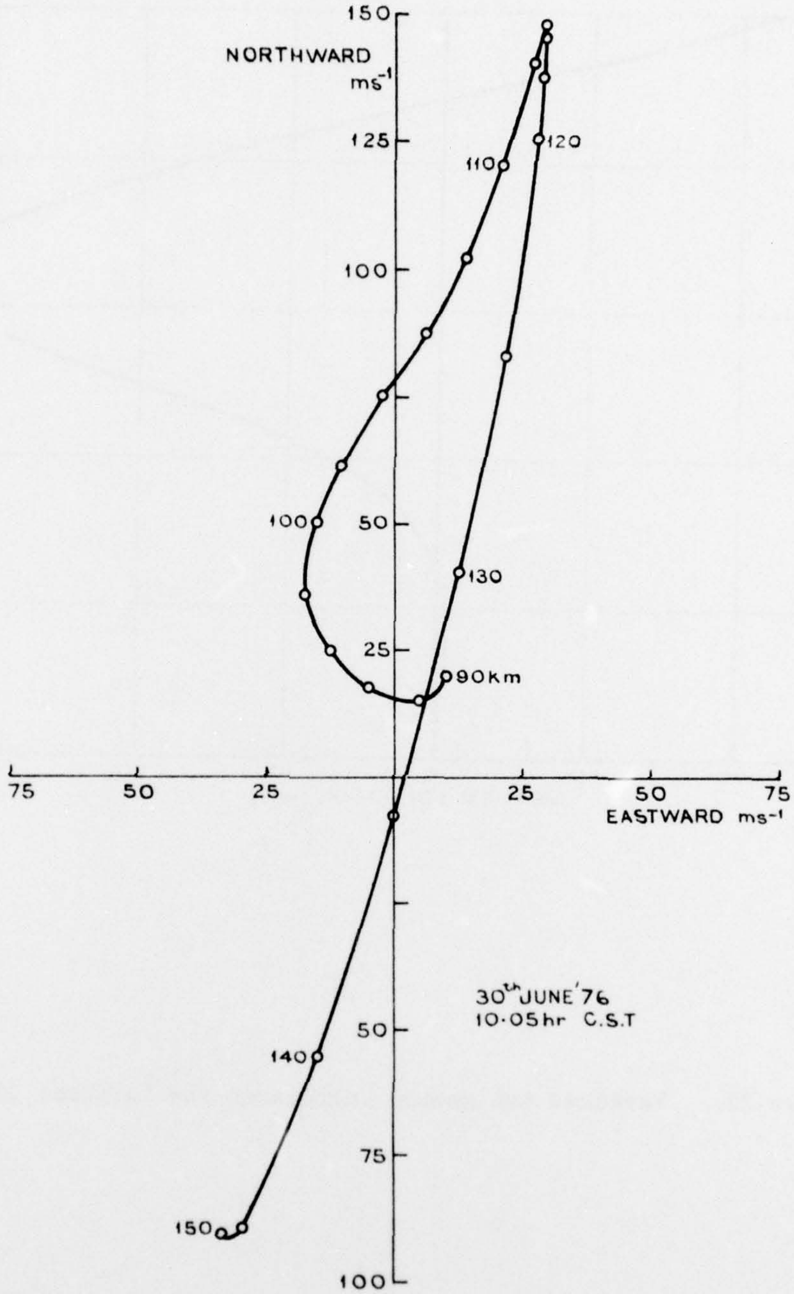

Figure 21. Wind hodograph for Lorikeet 2015

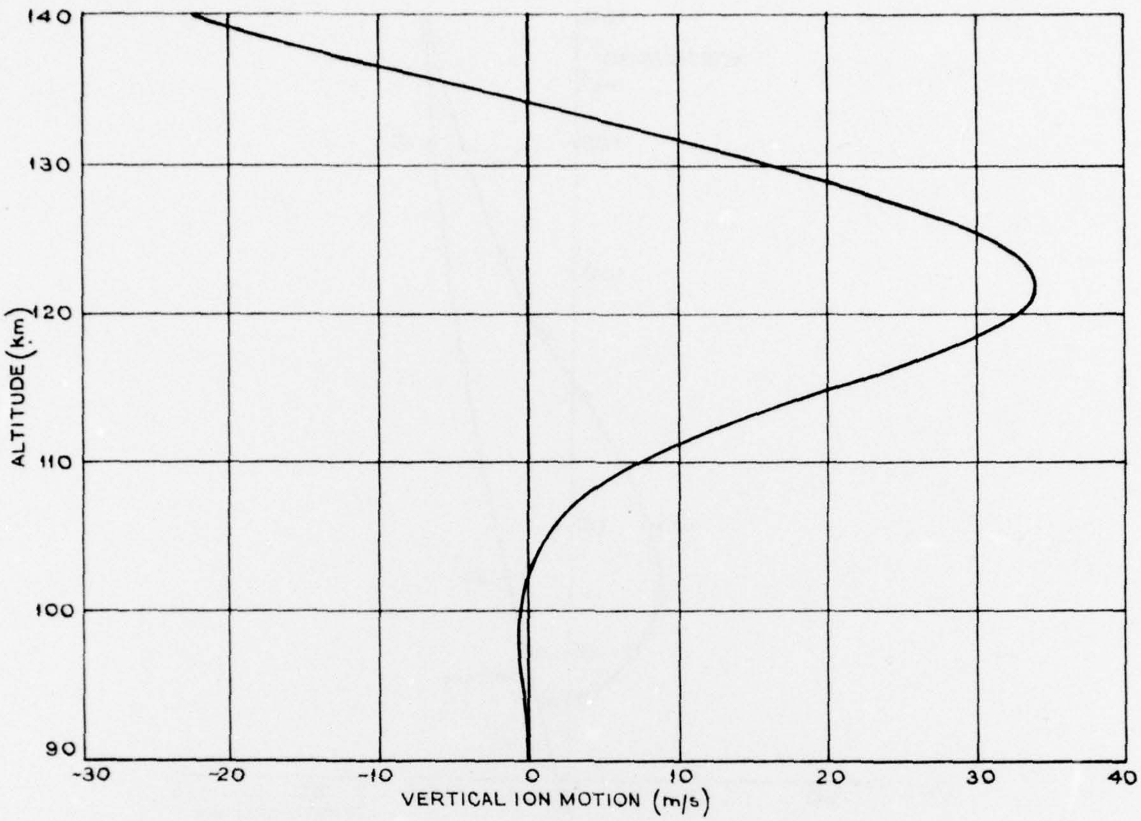

Figure 22. Vertical ion motion calculated for Lorikeet 2015

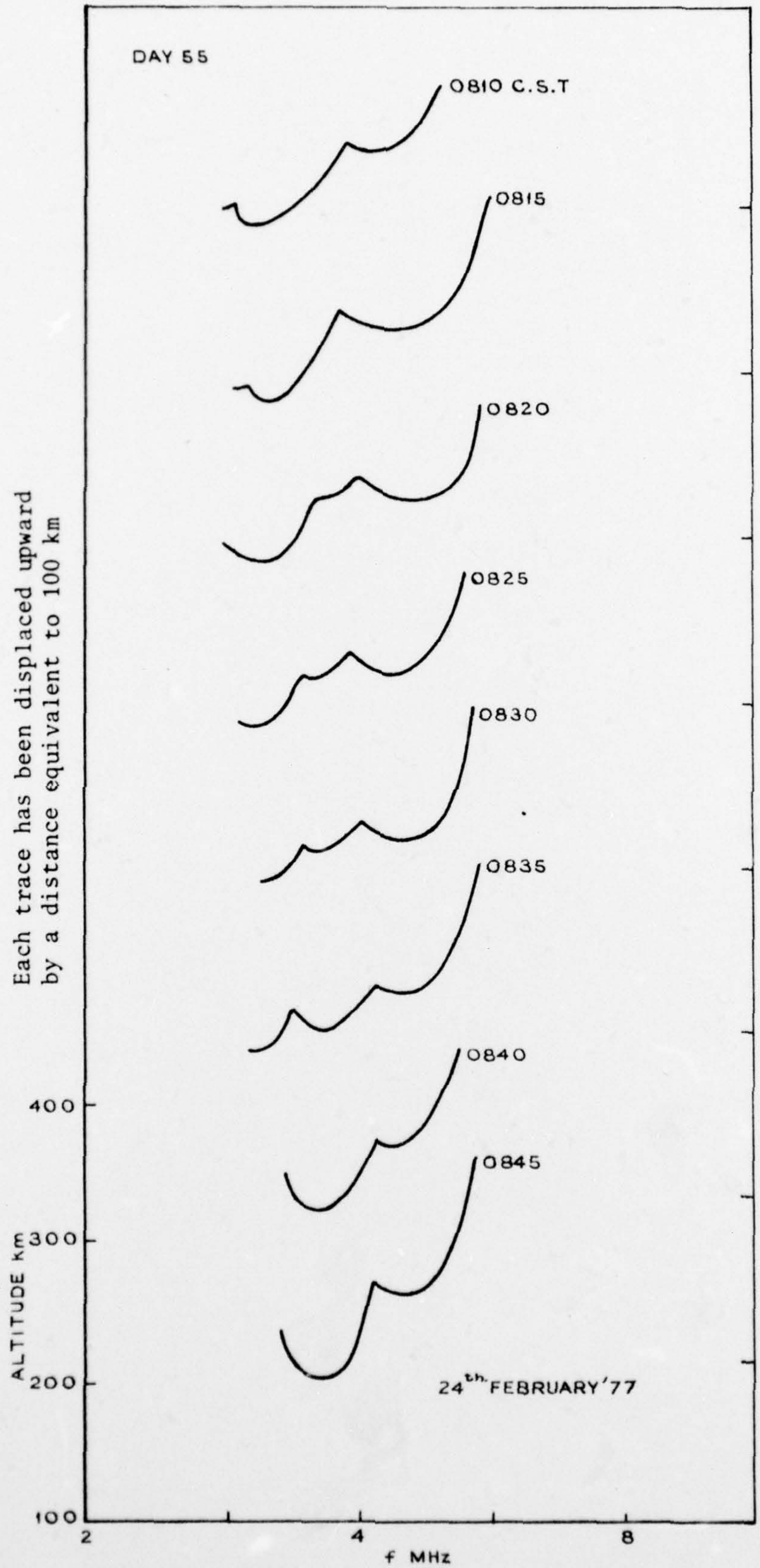

Figure 23. Ionogram traces showing T.I.D.S. between times of C3010 and L2011

DISTRIBUTION

EXTERNAL

	Copy No.
In Argentina	
Observatorio Astronomico, Marquezado, San Juan	
(Attention: Dr. A. Zaragota)	1
In Belgium	
Belgian Institute for Space Aeronomy, Brussel, B-1180	
(Attention: Dr. M. Ackerman)	2
In Canada	
University of Toronto	
(Attention: Prof. C.O. Hines)	3
In Federal Republic of Germany	
Max-Planck Institute for Extraterrestial Physics, Garchingb, Munich, 8046	
(Attention: Dr. G. Haerendel)	4
(Attention: Dr. E. Rieger)	5
In France	
Centre National de la Recherche Scientifique Service d'Aeronomie	
(Attention: Mlle. M.L. Chanin)	6
(Attention: Dr. J. Barat)	7
ELDO/ESRO	8
Group de Recherches Ionospheriques, C.N.E.T., Station Pierre Le jay, Garchy (Nievre)	
(Attention: M.A. Haubert)	9
In India	
Physical Research Laboratories, Ahmedabad 9	
(Attention: Prof. P.R. Pisharoty)	10
In Italy	
Intituto di Fisica Atmosfera, Bologna, 40126	
(Attention: Prof. F. Verniana)	11
In Japan	
Institute of Physics, University of Tokyo	
(Attention: J. Nakamura)	12
In New Zealand	
D.S.I.R. Wellington	13

		Copy No.
University of Canterbury		
	(Attention: Prof. L.F. Phillips)	14
	(Attention: Dr.G.J. Fraser)	15
	(Attention: Mr. P.J. Wilkinson)	16
University of Auckland/Radio Research Centre		
	(Attention: Mr. D.A. Price)	17
In Norway		
The Auroral Observatory, Tromso		
	(Attention: Mr. O. Harang)	18
In Pakistan		
Director, Pakistan Space and Upper Atmosphere Research Committee, Karachi		
	(Attention: Dr. M. Shafi Ahmad)	19
In United States of America		
Counsellor, Defence Science, Washington D.C.		20
N.A.S.A.		
	Headquarters, Washington D.C., 20546 (Attention: Mr. M. Dubin)	21
	Lewis Research Centre, Cleveland, Ohio	22
	Langley Research Centre, Hampton, Va (Attention: Dr. D. Adamson)	23
	Goddard Space Flight Centre, Greenbelt, Maryland, 20771 (Attention: Dr. W. Nordberg)	24
Library of Congress		25
Air Force Cambridge Research Laboratories, Hanscom Field, Massachusetts, 01730		
	(Attention: Dr. N.W. Rosenberg)	26
	(Attention: Dr. D. Golomb)	27
	(Attention: Dr. M.A. MacLeod)	28
Ballistics Research Laboratories, Aberdeen Proving Ground, Maryland, 21005		
	(Attention: Dr. C.H. Murphy)	29
Georgia Institute of Technology, Atlanta, Georgia, 30332		
	(Attention: Dr. R.G. Roper)	30
	(Attention: Dr. C.G. Justus)	31
G.C.A. Technology Division, Bedford, Massachusetts, 01730		
	(Attention: Dr. F.F. Marmo)	32
	(Attention: Dr. H. Bedinger)	33

	Copy No.
National Centre for Atmospheric Research, Boulder Colorado, 80302	34
Sandia Laboratories, Albuquerque, New Mexico, 87115	
(Attention: Dr. L.B. Smith)	35
Space Research Institute, Northfield, Vermont, 05663	
(Attention: Dr. G.V. Bull)	36
University of Illinois, Urbana, Illinois, 61801	
(Attention: Prof. S.A. Bowhill, Department of Electrical Engineering)	37
Geophysical Institute, University of Alaska, Fairbanks	38
In United Kingdom	
Defence Science and Technology Representative, Australia House, London	39
Ministry of Defence, London	
AD/TGW2	40
TGW25, Weapons Research Establishment Representative	41
The Chairman, Rockets Working Group	
Design of Experiments Sub-Committee of the British National Committee for Space Research	42
Royal Aircraft Establishment	
(Attention: Head of Space Department)	43
(Attention: Library)	44
Admiralty Centre for Scientific Information and Liaison	45
National Lending Library of Science and Technology	46
University of Belfast, Department of Physics	
(Attention: Dr. A. Dalgarno)	47
University of Sheffield, Department of Physics	
(Attention: Professor T.R. Kaiser)	48
University College, London	
(Attention: Professor G.V. Groves)	49
(Attention: Dr. D. Rees)	50
University of Southampton, Department of Physics	
(Attention: Dr. Pamela Rothwell)	51
University of Sussex, Department of Physics	
(Attention: Professor G. Martelli)	52
Appelton Laboratory, Ditton Park, Slaugh, Bucks	53

	Copy No.
In Australia	
Department of Defence	
Chief Defence Scientist	54
Controller, Programme Planning and Policy	55
Army Scientific Adviser	56
Air Force Scientific Adviser	57
Naval Scientific Adviser	58
Executive Controller, Australian Defence Scientific Service	59
Superintendent, Defence Science Administration Division	60
Assistant Secretary, Defence and Information Services (for microfilming)	61
Superintendent, Central Studies Establishment	62
Aeronautical Research Laboratories, Library	63
Materials Research Laboratories, Library	64
Defence Library, Campbell Park	65
Director, Joint Intelligence Organisation (DDSTI)	66
Australian National Library (through AS/DIS)	67
Department of Science	
Director Antarctic Division, Melbourne	68
Head of BDRSS, Salisbury	69
N.A.S.A. Senior Scientific Representative, Canberra	70
C.S.I.R.O. Division of Physics, Narrabri, N.S.W.	
(Attention: Dr. E.B. Armstrong)	71
Flinders University, Bedford Park, S.A.	
(Attention: Head of School of Physical Sciences)	72
(Attention: Head of Department of Meteorology)	73
La Trobe University, Bundoora, Victoria	
(Attention: Head of Department of Physics)	74
Mount Stromlo Observatory, Canberra	
(Attention: Director)	75
University of Adelaide, South Australia	
(Attention: Head of Department of Physics)	76
(Attention: Dr. B. Briggs)	77
(Attention: Dr. R.A. Vincent)	78
University of Melbourne, Parkville, Victoria	
(Attention: Head of Department of Physics)	79
University of Queensland, St. Lucia, Queensland	
(Attention: Professor D. Whitehead)	80

	Copy No.
University of Western Australia, Crawley, W.A. (Attention: Head of Department of Physics)	81
INTERNAL	
Director	82
Chief Superintendent, Weapons Research and Development Wing	83
Chief Superintendent, Applied Physics Wing	84
Superintendent, Aerospace Division	85
Superintendent, Propulsion and Marine Physics Division	86
Superintendent, Systems Assessment Division	87
Principal Officer, Combustion and Explosives Group	88
Principal Officer, Field Experiments Group	89
Principal Officer, Flight Research Group	90
Principal Officer, Upper Atmosphere Research Group	91
Principal Officer, Ionospheric Studies Group	92
Principal Officer, Tropospheric Studies Group	93
Principal Officer, Underwater Detection Group	94
Principal Officer, Marine Physics Group	95
Authors	96 - 98
A.D. Library	99 - 100
Library, W.R.E.	101 - 102
Spares	103 - 110